Cell Stem Cell

Clinical and Translational Report

Development of human induced pluripotent stem cell-derived ovarian support cells as a clinical-grade product for *in vitro* fertilization

Graphical abstract

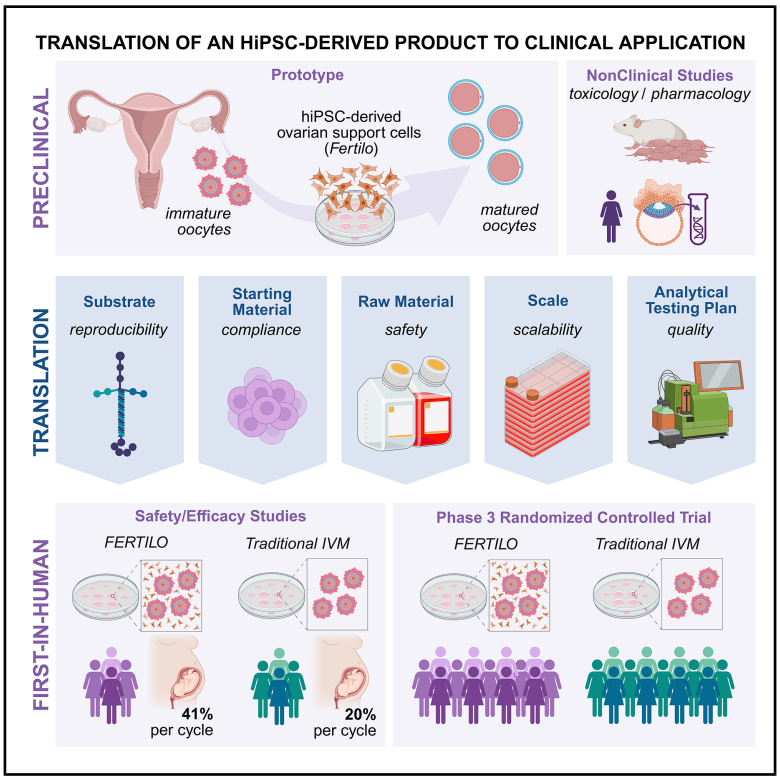

Highlights

- TF-mediated hiPSC differentiation generates OSCs that improve the IVM of human oocytes
- Raw material upgrades promote the reproducibility and consistency of OSC manufacturing
- Quality, safety, and potency assessments establish the clinical readiness of *Fertilo*
- Clinical application of *Fertilo* improves the outcomes of minimal stimulation IVM

Authors

Bruna Paulsen, Ferran Barrachina, Sabrina Piechota, ..., David F. Albertini, Michel De Vos, Christian C. Kramme

Correspondence

christian@gametogen.com

In brief

Paulsen et al. present the process development and clinical application of an hiPSC-derived OSC product, *Fertilo*. They describe the raw material upgrades, process consistency and reproducibility, and analytical assessment required for the generation of a clinically suitable product, as well as favorable outcomes from the first-in-human application of *Fertilo*.

Paulsen et al., 2026, Cell Stem Cell *33*, 1–15
February 5, 2026
https://doi.org/10.1016/j.stem.2025.12.020

CellPress

Cell Stem Cell

CellPress
OPEN ACCESS

Clinical and Translational Report

Development of human induced pluripotent stem cell-derived ovarian support cells as a clinical-grade product for *in vitro* fertilization

Bruna Paulsen,[1] Ferran Barrachina,[1] Sabrina Piechota,[1] Alexander D. Noblett,[1] Mark Johnson,[1] Simone Kats,[1] Cassandra Lew,[1] Maria Marchante,[1] Alexandra B. Figueroa,[1] Itzel Garcia Granada,[2] Elizabeth Ingalls Lopez,[2] Erick Martinez,[2] Paula Ricra,[3] Camila Carlos,[3] Jazmin Meza,[3] Wendy Montanchez,[3] Pilar Pino,[3] Cesar Reategui,[3] Enrique Noriega,[3] Alicia Elias,[3] Luis Noriega-Portella,[3] Gus Haddad,[1] Dina Radenkovic,[1] Eugenia Moran,[2] Pamela Villanueva,[3] Jose Guiterrez,[2] Luis Guzman,[3] Pietro Bortolleto,[4] David F. Albertini,[5] Michel De Vos,[6] and Christian C. Kramme[1,7,*]

[1]Gameto Inc., New York, NY, USA
[2]Fertilidad Integral, Mexico City, Mexico
[3]Pranor Clinic, Lima, Peru
[4]Boston IVF, Boston, MA, USA
[5]Bedford Research Foundation, Bedford, MA, USA
[6]Brussels IVF, Universitair Ziekenhuis Brussel, Vrije Universiteit Brussel, Brussels, Belgium
[7]Lead contact
*Correspondence: christian@gametogen.com
https://doi.org/10.1016/j.stem.2025.12.020

SUMMARY

Human induced pluripotent stem cells (hiPSCs) show promise in the development of novel strategies to alleviate reproductive diseases and improve reproductive outcomes. Here, we detail the clinical development and application of an ovarian support cell (OSC) product, Fertilo, to improve the *in vitro* maturation (IVM) of human oocytes. First, we demonstrate that transcription factor-mediated hiPSC differentiation produces OSCs that improve the oocyte MII maturation rate. To support clinical application, we describe raw material upgrades and the generation of clinically suitable hiPSC seed and master cell banks, with transcriptomic analysis of resultant OSCs showing consistent and reproducible outcomes. Next, we detail analytical release testing and development of a murine oocyte maturation assay to assess product potency. Finally, application of *Fertilo* in a longitudinal cohort analysis shows improvement in key outcomes, compared with traditional IVM. Our findings demonstrate the first-time clinical development and application of an hiPSC-derived product to promote successful reproductive outcomes.

INTRODUCTION

Reproductive diseases such as endometriosis, polycystic ovary syndrome (PCOS), and infertility affect over 10% of the population and impose substantial healthcare and economic burdens.[1–4] Despite the prevalence and clinical significance of these diseases, therapeutic development in reproductive medicine has lagged,[5,6] contributing to healthcare disparities and hindering innovation. Human induced pluripotent stem cells (hiPSCs) offer new opportunities for reproductive health based on their potential to be differentiated into any cell type in the body, including ovarian support cells (OSCs) with phenotypic and functional similarities to somatic granulosa cells within the ovarian follicle.[7–10] Modulation of the expression of key transcription factors (TFs) involved in granulosa cell specification enables the efficient differentiation of hiPSCs into mature OSCs.[8] Differentiated OSCs mimic the ovarian environment *in vitro*, constituting a platform with diverse applications from investigation of gamete-somatic cell interactions to clinical applications, such as the *in vitro* maturation (IVM) of oocytes, *in vitro* gametogenesis, disease modeling, and drug screening.

While conventional *in vitro* fertilization (IVF) is a widely adopted assisted reproductive technology (ART), it relies on high-dose gonadotropin administration and predisposes women to ovarian hyperstimulation syndrome (OHSS), which can be particularly dangerous for women with a high risk, including patients contraindicated for gonadotropin stimulation, patients with PCOS, or other hyper-responders. Meanwhile, IVM provides a milder alternative as it is performed under a minimal stimulation protocol, which drastically reduces the amount and duration of hormone administration. However, despite being less burdensome and painful, compared with conventional IVF,[11] IVM has been limited by poor embryological and clinical outcomes.[12–14] Traditional IVM involves the culture of immature oocytes in culture media with supplemental growth factors and hormones. Although these conditions provide some additives needed for oocyte

Please cite this article in press as: Paulsen et al., Development of human induced pluripotent stem cell-derived ovarian support cells as a clinical-grade product for *in vitro* fertilization, Cell Stem Cell (2025), https://doi.org/10.1016/j.stem.2025.12.020

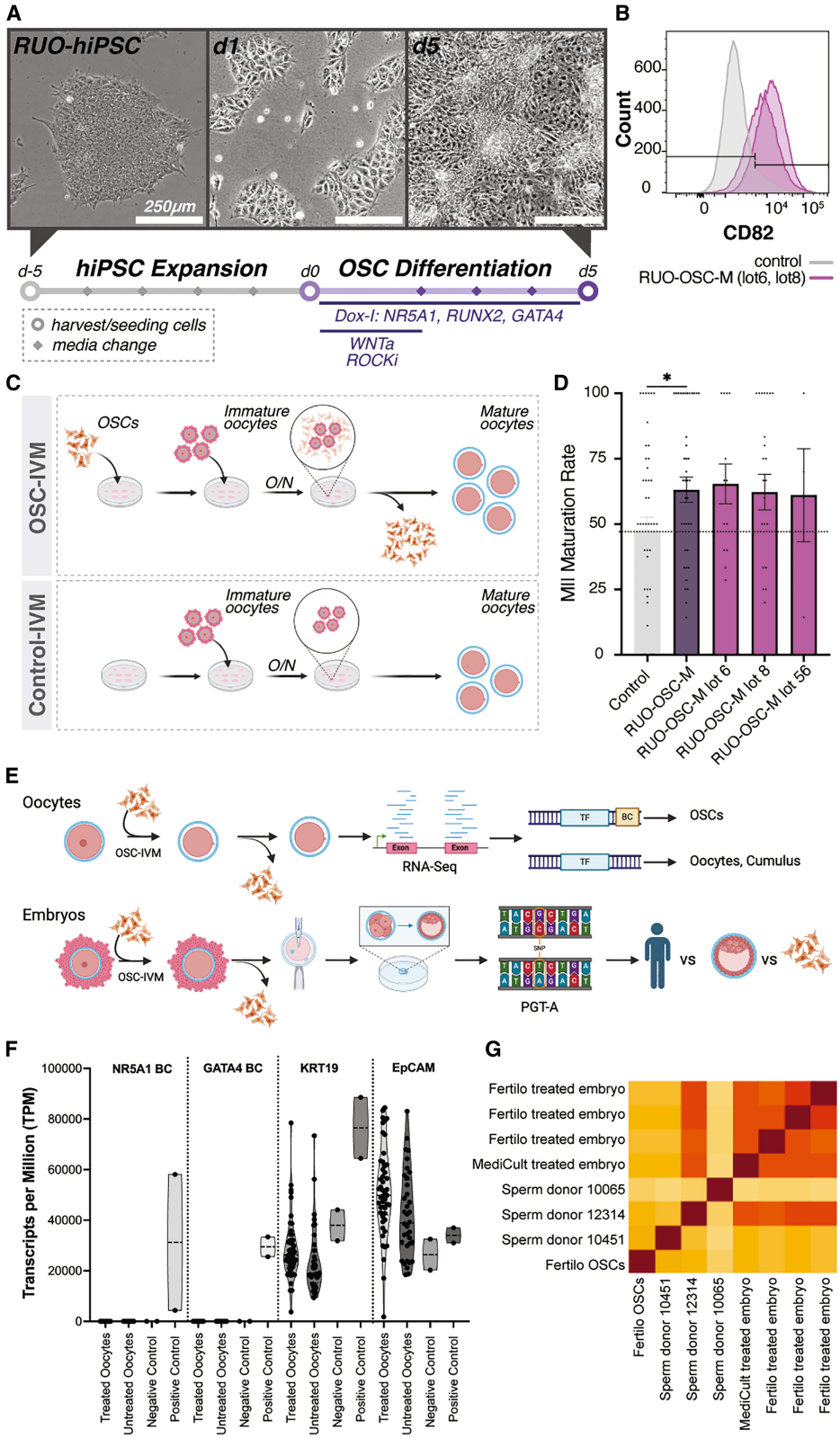

Figure 1. TF-mediated hiPSC differentiation to generate OSCs that improve the rate of MII oocyte maturation

(A) Timeline and representative images of RUO-hiPSC expansion and OSC differentiation onto Matrigel (M). Images on day 5 of hiPSC expansion and days 1 and 5 of OSC differentiation. Scale bar, 250 μm.

(legend continued on next page)

Please cite this article in press as: Paulsen et al., Development of human induced pluripotent stem cell-derived ovarian support cells as a clinical-grade product for *in vitro* fertilization, Cell Stem Cell (2025), https://doi.org/10.1016/j.stem.2025.12.020

maturation, this culture method is static and unable to dynamically respond throughout treatment. However, the addition of ovarian cells to IVM culture allows for dynamic signaling and response with the changing needs of the maturing oocyte.[15,16] While primary granulosa cell co-culture can improve IVM outcomes,[15,16] there are several barriers to the implementation of this practice in clinical settings. Specifically, primary granulosa cells are derived and isolated from human tissue, which is a finite and non-renewable resource that has inherent variability. hiPSC-derived OSCs offer a sustainable and feasible alternative to primary granulosa cells, and recent studies have demonstrated that hiPSC-derived OSC co-culture, via a method called OSC-IVM, can improve oocyte maturation and euploid blastocyst formation.[17,18]

The ability to recreate the ovarian microenvironment in a dish, by direct co-culture of OSCs and oocytes, supports oocyte maturation *in vitro* and improves IVM outcomes.[17–19] Not only does OSC-IVM improve oocyte maturation and blastocyst formation rates (BFRs), but resultant mature oocytes demonstrated more transcriptomic similarity to *in vivo*-maturated oocytes than those matured via traditional IVM, and the epigenetic profiles of blastocysts exhibited the same trend.[17,18] In a multigenerational murine study, OSC-IVM did not lead to reprotoxicity, and the implantation of resultant embryos led to healthy live births.[20] There were also no significant differences in the live birth rates, sex ratio, development, or behavior of F1 and F2 offspring, following OSC-IVM.[20] Although previous studies demonstrated the promise of OSC-IVM, clinical application of allogeneic OSCs for *ex vivo* gamete co-culture requires a meticulous approach to address several process challenges.

This manuscript details the strategic development of an hiPSC-derived OSC product, *Fertilo*, through clinical translation. Following initial proof of concept experiments, product development studies with the implementation of high-grade raw materials and a clinically suitable hiPSC line engineered to generate clinical-grade (CG) OSCs led to the generation of consistent and efficacious OSC populations. Then, several OSC lots were verified by analytical release testing and a murine oocyte maturation assay (MOMA) to assess potency. In the first-in-human study of OSCs, *Fertilo* improved euploid blastocyst formation and ongoing pregnancy rates, compared with traditional IVM, in addition to multiple healthy live births. This study is the first to demonstrate the end-to-end manufacturing, product release, and application of a clinical product developed from hiPSCs. Notably, this product is the first hiPSC-derived therapy developed for use in IVF, the first hiPSC-derived product to enter phase 3 clinical trials in the United States, and the first product derived via TF-directed differentiation of hiPSCs to enter phase 3 trials globally.

RESULTS

TF-directed hiPSC differentiation generates OSCs that improve MII oocyte maturation

Fertilo is a cell-based product composed of engineered hiPSC-derived OSCs utilized for the IVM of human oocytes, after which mature MII oocytes are isolated and used in standard IVF. To guide clinical translation of *Fertilo* and establish good manufacturing practice (GMP) and preclinical safety and efficacy assessment, a quality target product profile (QTPP) was established (Table S1), followed by process development and preclinical studies to define the differentiation protocol, efficacy in a therapeutic model, and the toxicological profile.[8,17,20]

Previous studies demonstrated that inducible expression of key TFs involved in granulosa cell specification (*NR5A1*, *RUNX2*, and *GATA4*) drives hiPSC differentiation into mature OSCs with phenotypic and functional similarities to somatic granulosa cells of the ovary.[8] To evaluate the phenotypic consistency, six independent batches of OSCs were generated from the previously described research-use-only (RUO)-hiPSC line (Table S2).[8] After 5 days of induction on Matrigel, RUO-hiPSCs multiplied 5.63 ± 2.85 times and acquired human granulosa-like cell (GC) morphology, such as clusters of cells with spiky edges and granules in the cell body (Figure 1A) and expressed CD82, a marker associated with granulosa cell fate,[8,21] indicating successful differentiation (Figure 1B). When applied in IVM co-culture with human oocytes, all RUO-OSC-M batches increased MII oocyte maturation rates, compared with the control group ($p = 0.029$, lot 6/control: 1.37, lot 8/control: 1.31, lot 56/control: 1.28) (Figures 1C and 1D).

A key safety aspect of *Fertilo* is the exclusive *ex vivo* nature of the application and elimination of OSCs, which prevents allogeneic cell transfer to patients or progeny. To verify OSC removal, human oocytes and embryos post-treatment were assessed

(B) Flow cytometry analysis of the granulosa cell marker, CD82, in RUO-OSC-M lots and the negative (unstained) control.
(C) Schematic representation of the two IVM conditions: the control-IVM group containing IVM media only vs. the OSC-IVM group constituted by IVM media supplemented with OSCs.
(D) MII maturation rate in control-IVM (gray) vs. OSC-IVM groups. "RUO-OSC-M" displays the combined oocyte maturation rates of three separate OSC batches (RUO-OSC-M lots 6, 8, and 56). Statistical differences were evaluated using unpaired *t* tests, compared with control, with a $p < 0.05$ considered statistically significant. Data are shown as the mean ± SEM ($p = 0.0288$, lot 6 vs. control:1.37, lot 8 vs. control: 1.31, lot 56 vs. control: 1.28). The number of donors (*N*) from whom oocytes (*n*) were collected in each group is provided in Table S10.
(E) Flowchart demonstrating the testing strategy to verify OSC removal from post-treatment human oocytes and embryos. Barcode-seq analysis was performed on post-treatment oocytes, and SNP-based PGT-A analysis was performed on post-treatment embryos.
(F) Barcode-seq analysis of 48 post-treatment oocytes. Analysis of the presence of barcodes (as transcripts per million) for OSCs with synthetic TFs and the reference genes KRT19 and EpCAM. Analysis was performed using both OSC line data (bulk RNA-seq) and post-IVM oocyte cell data (low input RNA-seq). Transcript capture of reference genes shows high read depth and quality library preparation.
(G) SNP-based PGT-A analysis of post-treatment embryos, sperm donor samples, and *Fertilo* OSCs. Patient oocytes were treated with *Fertilo* or IVM media. Mature oocytes were fertilized using sperm from sperm donor 12314, resulting in 4 blastocysts sent for PGT-A analysis, 3 derived from *Fertilo* treatment and 1 derived from IVM treatment. SNP detection via PGT-A analysis was performed and included analysis of negative controls (sperm donor 10451 and sperm donor 10065), as well as a sample of *Fertilo* OSCs (GTO-101-Lot-006) and the fertilization partner (sperm donor 12314). The assay correctly identified the fertilization partner, with non-partner sperm showing no evidence of overlapping with embryo samples.

Please cite this article in press as: Paulsen et al., Development of human induced pluripotent stem cell-derived ovarian support cells as a clinical-grade product for *in vitro* fertilization, Cell Stem Cell (2025), https://doi.org/10.1016/j.stem.2025.12.020

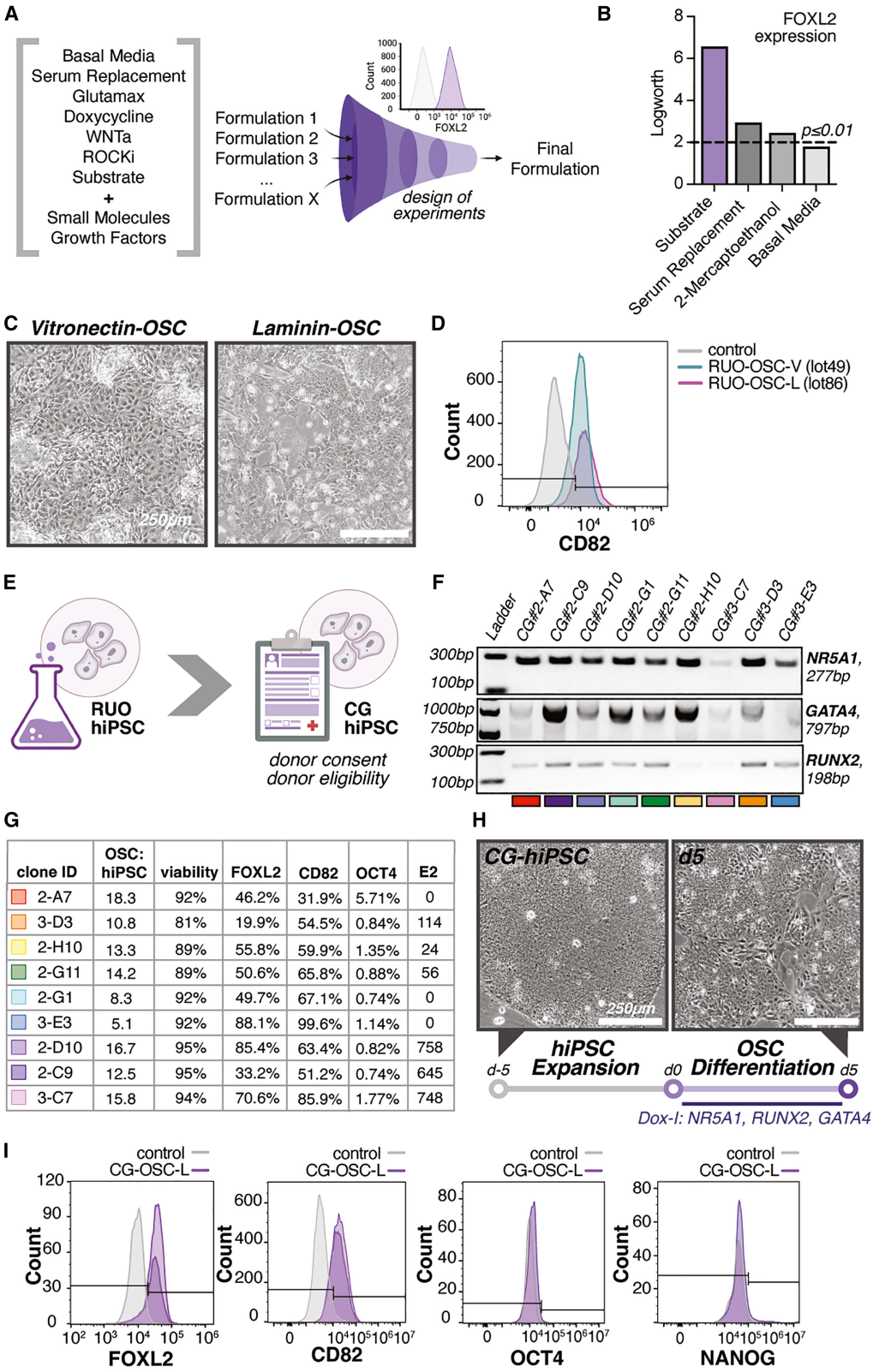

clone ID	OSC: hiPSC	viability	FOXL2	CD82	OCT4	E2
2-A7	18.3	92%	46.2%	31.9%	5.71%	0
3-D3	10.8	81%	19.9%	54.5%	0.84%	114
2-H10	13.3	89%	55.8%	59.9%	1.35%	24
2-G11	14.2	89%	50.6%	65.8%	0.88%	56
2-G1	8.3	92%	49.7%	67.1%	0.74%	0
3-E3	5.1	92%	88.1%	99.6%	1.14%	0
2-D10	16.7	95%	85.4%	63.4%	0.82%	758
2-C9	12.5	95%	33.2%	51.2%	0.74%	645
3-C7	15.8	94%	70.6%	85.9%	1.77%	748

(legend on next page)

Please cite this article in press as: Paulsen et al., Development of human induced pluripotent stem cell-derived ovarian support cells as a clinical-grade product for *in vitro* fertilization, Cell Stem Cell (2025), https://doi.org/10.1016/j.stem.2025.12.020

using next-generation sequencing (NGS) targeting the 20-bp barcode in the 3′ UTR of exogenous TFs unique to OSCs (Figure 1E).[18,22] Barcode sequencing (Barcode-seq) analysis of 48 post-treatment oocytes detected no residual OSCs, with high specificity and sensitivity demonstrated in controls (positive: OSCs, $n = 2$; negative: untreated oocytes, $n = 36$; cumulus cells, $n = 2$) (Figure 1F). Additionally, single-nucleotide polymorphism (SNP)-based preimplantation genetic testing for aneuploidy (PGT-A) analysis of 26 blastocysts derived from OSC-treated oocytes revealed no OSC-derived genetic material (Figure 1G), supporting the safety of OSC-IVM.

Translation of the protocol toward clinical manufacturing with HQ clinically suitable raw materials

Although pure and functional OSCs were generated, initial manufacturing relied on research-grade raw materials unsuitable for clinical use. To assess whether higher-quality alternatives would alter OSC purity or potency, a risk assessment was conducted with a systematic evaluation of differentiation outcomes. A list of critical factors was compiled from the literature, and appropriate test concentrations were identified (Table S3). To investigate the effects of multiple variables at once, a design of experiments (DOE) approach was applied to optimize FOXL2 expression, which indicates OSC specification, and viability (Figure 2A). These results demonstrated that the substrate had a clear and strong influence on FOXL2 expression (Figure 2B, $p \leq 0.01$), exceeding all other factors.

Based on this result, and the lot-to-lot variability of Matrigel, two animal origin-free extracellular matrix substrates appropriate for clinical translation—laminin and vitronectin—were evaluated. Differentiation of the RUO-hiPSC line on both substrates produced OSCs expressing the granulosa cell marker CD82, with subtle morphological differences between groups (Figure 2D). Vitronectin-OSCs (RUO-OSC-V) exhibited a larger cell body and were organized in sparse clusters of cells, while laminin-OSCs (RUO-OSC-L) were smaller and organized in compact groups (Figure 2C). Analytical testing demonstrated that RUO-OSC-L lots had more cells expressing OSC markers, increased cell viability, and significantly reduced expression of the hiPSC marker, TRA-1-60, compared with RUO-OSC-V lots, indicating improved differentiation efficiency and purity (Table 1).

To generate a CG starting material, an hiPSC line derived from an allogeneic female donor was genetically engineered to harbor inducible versions of three TFs, *NR5A1*, *RUNX2*, and *GATA4* (Figure 2E).[8] Individual clones were generated by limiting dilution of the pooled engineered population and expanding into seed banks that underwent initial screening by genotyping PCR to confirm TF integration; nine harbored the desired TF combination (Figure 2F). The differentiation capacity of the nine clones was assessed via flow cytometry based on FOXL2 and CD82 expression, with few residual hiPSCs, as indicated by POU5F1 (OCT4) expression, after 5 days. All clones were positive for both OSC markers with low or null hiPSC marker expression, indicating successful differentiation (Figures 2G and S2B).

On the 5th day after differentiation, the steroidogenic function of clones was assessed, with clones 2-D10 and 3-C7 showing the greatest steroidogenic responses (Figures 2G and S2C). In addition, bulk RNA-seq showed that all clones robustly expressed granulosa cell markers (*FOXL2*, *STAR*, and *GJA5*), as well as genes related to signaling pathways associated with oocyte-granulosa cell interactions (*NOTCH3*, *HES1*, *ID3*, and *KITLG*) (Figure S2E).[13] Overall, clone 2-D10 was the top candidate (hereafter referred to as CG-hiPSC), based on high FOXL2 and CD82 expression, few residual hiPSCs, high E2 production, high cell viability at harvest, and the highest ratio of OSCs to hiPSCs seeded at the start of differentiation (OSC:hiPSC) (Figure 2G).

Using the updated protocol and higher-quality alternative raw materials, three independent CG-OSC batches (CG-OSC-L lot 88, lot 90, and lot 116) were generated. To evaluate the potential for scalability, the first two lots of CG-OSCs (lot 88 and lot 90) were differentiated onto 55-cm^2 dishes (Table S2), and CG-OSC-L lot 116 was differentiated onto 175-cm^2 dishes. All lots exhibited GC morphology (Figure 2H), with OSC identity confirmed based on FOXL2 and CD82 expression and with purity verified based on the absence of hiPSC marker expression (Figures 2I and S3). Viability at harvest remained high, averaging 97.17% ± 0.56% among the three batches. The OSC:hiPSC ratio was similar to that achieved with the RUO-hiPSC line when differentiated over laminin-521 (14.83 ± 4.48), averaging 11.41 ± 2.19 for the first two batches (lot 88 and lot 90, Table S2). Interestingly, differentiation of CG-OSC-L lot 116 onto larger dishes (175 cm^2) led to a considerably higher OSC:hiPSC ratio (30.7, Table S2), suggesting notable scalability potential.

TF-directed hiPSC differentiation, using CG materials, leads to OSCs with consistent cellular outcomes

To evaluate reproducibility and process consistency, single-cell RNA sequencing (scRNA-seq) was performed on RUO-OSC-M, RUO-OSC-V, RUO-OSC-L, and CG-OSC-L lots (Figure 3A). scRNA-seq analysis revealed three distinct clusters: less mature GCs (early GCs), more mature GCs (GCs), and "others." Early GC and GC clusters robustly expressed markers of granulosa

Figure 2. Translation of the protocol toward clinical manufacturing using HQ clinically suitable raw materials

(A) Schematic of the DOE strategy to optimize the manufacturing process.

(B) Barplot of logworth values of DOE main effect on FOXL2 expression. The dashed line indicates $p \leq 0.01$. Information about the data analysis can be found in the DOE section in the STAR Methods.

(C) Images of OSCs in culture on day 5 of differentiation carried out on vitronectin vs. laminin-521. Scale bar, 250 μm.

(D) Flow cytometry analysis of the expression of CD82 in the control, RUO-OSC-V, and RUO-OSC-L.

(E) Schematics of requirements for generation of a CG-hiPSC line.

(F) Image of genotyping PCR gel confirming the presence of all three TFs (*NR5A1*, *GATA4*, and *RUNX2*) in each of the nine clones.

(G) Chart displaying the 9 clones and 4 markers: FOXL2, CD82, OCT4, and E2. The chart displays the ratio of the presence of OSC markers (FOXL2 and CD82) in relation to the hiPSC markers (OCT4 and E2) in each clone, the viability of each sample, and the amount of each marker present in each sample as a percentage.

(H) Images of CG-OSCs (lot 90) grown on laminin on day 5 of hiPSC expansion and day 5 of OSC differentiation. Scale bar, 250 μm.

(I) Flow cytometry analysis of OSC markers: FOXL2 and CD82. Expression levels of these markers were evaluated in CG-OSC-L against the negative control.

Please cite this article in press as: Paulsen et al., Development of human induced pluripotent stem cell-derived ovarian support cells as a clinical-grade product for *in vitro* fertilization, Cell Stem Cell (2025), https://doi.org/10.1016/j.stem.2025.12.020

Table 1. Analytical assessment of clinical attributes

Production lot	OSC markers (CD82+, FOXL2+)	Viability	Residual hiPSCs (TRA-1-60+)	Cell count	BFR
RUO-OSC-V lot 41	CD82+: 51.1%; FOXL2+: NT	81.7%	31.1%	NT	NT
RUO-OSC-V lot 49	CD82+: 57.7%; FOXL2+: NT	82.8%	72.5%	NT	NT
RUO-OSC-L lot 77	CD82+: 50.8%; FOXL2+: NT	86.5%	3.5%	NT	NT
RUO-OSC-L lot 86	CD82+: 87.4%; FOXL2+: NT	86.2%	1.3%	NT	NT
CG-OSC-L lot 88	CD82+: 78.3%; FOXL2+: 71.2%	90.20%	0.01%	NT	NT
CG-OSC-L lot 90	CD82+: 74.1%; FOXL2+: 92.1%	91.20%	0.03%	NT	NT
CG-OSC-L lot 116	CD82+: 97.4%; FOXL2+: 99.5%	94.63%	0.08%	NT	NT
CG-OSC-L lot 180	CD82+: 94.2%; FOXL2+: 99.2%	94.37%	0.46%	NT	NT
CG-OSC-L lot 182	CD82+: 98.5%; FOXL2+: 90.8%	88.40%	0.87%	NT	NT
Fertilo lot GA03-24-TR001	CD82+: 98.3%; FOXL2+: 96.7%	$\geq$ 87.4%	NT	$\geq 3.88 \times 10^5$ viable cells/vial	82.6%
Fertilo lot GA03-24-TR001; 5 min pot-thaw	CD82+: 91.3%; FOXL2+: 96.0%	94.0%	NT	3.72×10^5 viable cells/vial	80.0%
Fertilo lot GA03-24-TR001; 10 min pot-thaw	CD82+: 90.1%; FOXL2+: 95.4%	88.2%	NT	3.66×10^5 viable cells/vial	80.8%
Fertilo lot GA03-24-TR001; 15 min pot-thaw	CD82+: 92.7%; FOXL2+: 97.2%	90.1%	NT	3.71×10^5 viable cells/vial	87.1%
Fertilo lot GA03-24-TR001; 30 min in IVM media	CD82+: 89.1%; FOXL2+: 94.3%	84.5%	NT	8.52×10^4 viable cells/100 μL	80.0%
Fertilo lot GA03-24-TR001; 1 h in IVM media	CD82+: 90.3%; FOXL2+: 89.6%	80.2%	NT	8.64×10^4 viable cells/100 μL	87.0%
Fertilo lot GA03-24-TR001; 2 h in IVM media	CD82+: 91.0%; FOXL2+: 92.3%	81.3%	NT	8.10×10^4 viable cells/100 μL	90.2%
Fertilo lot GA03-24-TR001; 7 days shipping conditions	CD82+: 92.7%; FOXL2+: 99.8%	$\geq$86.3%	NT	$\geq 4.09 \times 10^5$ viable cells/vial	82.5%
Fertilo lot GA03-24-TR001; 6 months storage conditions	CD82+: 98.3%; FOXL2+: 96.7%	$\geq$82.8%	NT	$\geq 3.26 \times 10^5$ viable cells/vial	76.2%
Fertilo lot GA03-24-TR001; 12 months storage conditions	CD82+: 91.8%; FOXL2+: 97.1%	$\geq$84.2%	NT	$\geq 3.74 \times 10^5$ viable cells/vial	78.4%

NT, not tested.

cell fate, with early GCs also expressing pre-defined preGC-I/II marker genes (Figure S3A).[23] Cells classified as "others" were enriched in mitochondrial and ribosomal gene expression, typically associated with poor cell quality and a common artifact of scRNA-seq.[24]

RUO-OSC-M lots had variable distribution among the three major clusters, while RUO-OSC-V and RUO-OSC-L lots had more consistent outcomes, exhibiting an increased percentage of early GCs and GCs, respectively (Figures 3B and S3C). CG-OSC-L lots had a consistent high proportion of the mature population of GCs (>93%), with a decrease from 22% to <6% low-quality cells (others), compared with initial batches (Figures 3B and S3C). After implementation of the process modifications, there was increased expression of GC markers,[23] indicating improved purity and differentiation efficiency (Figure 3C). Furthermore, the functionality of the resultant OSCs was assessed via OSC-IVM with human oocytes, with all lots of OSCs leading to increased rates of MII maturation (Figures S3B and S3C).

To explore the potential mechanism of action, gene expression of key receptor-ligand components and growth factors was performed. Analysis of key receptor-ligand components revealed consistent enrichment of the receptors *TGFBR1*, *BMPR2*, and *NOTCH2/3*, as well as the ligand *EFNB2*, across OSC batches (Figure S3D). Of note, the NOTCH signaling pathway is involved in oocyte-GC crosstalk during folliculogenesis,[21] with high levels of *NOTCH2* and *NOTCH3* expression in cumulus cells positively correlated with IVF response.[25] Analysis of growth factors revealed enrichment in genes implicated in oocyte maturation and developmental competence acquisition, such as midkine (*MDK*), transforming growth factor (*TGF)B1*, epidermal growth factor (*EGF*), fibroblast growth factor 2 (*FGF2*), and *IGF2BP1/2/3*, thereby supporting a paracrine mechanism of action (Figure S3E).[26–31]

Complementary proteomics analysis of OSCs after 24 h *in vitro*, compared with OSCs prior to culture (0 h), showed that overexpressed proteins were enriched for functional profiling terms such as "transporter activity," "electron transfer activity," "aerobic respiration," and "cellular lipid metabolic process" (Figure S3F; Table S4B). Proteomic analysis of OSCs (0 h), compared with hiPSCs (0 h), showed that overexpressed proteins were enriched in functional profiling terms such as "cell-cell adhesion mediator activity," "cytoskeleton organization," and "focal adhesion" (Figure S3G; Table S4C). Among the proteins secreted by both the RUO and CG lines, relevant players associated with oocyte maturation and developmental

Please cite this article in press as: Paulsen et al., Development of human induced pluripotent stem cell-derived ovarian support cells as a clinical-grade product for *in vitro* fertilization, Cell Stem Cell (2025), https://doi.org/10.1016/j.stem.2025.12.020

CellPress
OPEN ACCESS

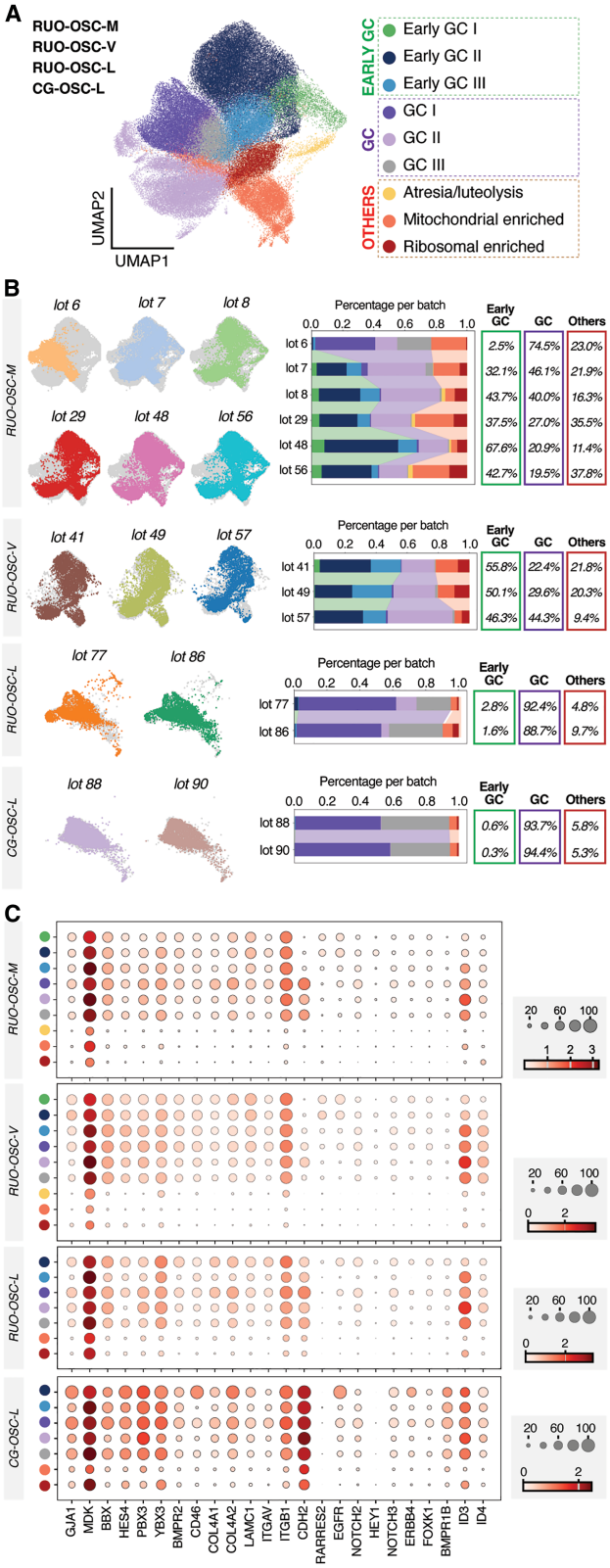

Figure 3. TF-mediated hiPSC differentiation by using CG materials leads to OSCs with consistent cellular outcomes

(A) Uniform manifold approximation and projection (UMAP) depicting all OSC subsets, including the RUO-OSC-M, RUO-OSC-V, RUO-OSC-L, and CG-OSC-L subsets.

(B) UMAP depicting each individual lot within the RUO-OSC-M, RUO-OSC-V, RUO-OSC-L, and CG-OSC-L subsets. Next to projections for each lot, a stacked bar plot depicts the amount of each cluster type found in each lot relative to each respective subset. The colors correspond to the UMAP cluster colors found in (A). Overall percentages per group are given to the right of the barplot.

(C) Dotplot depicting the expression of granulosa cell marker genes consistently expressed across GC clusters (GC consistent) and granulosa cell marker genes defined in previous studies (GC) in the RUO-OSC-M, RUO-OSC-V, RUO-OSC-L, and CG-OSC-L subsets.[18] The RUO-OSC-M dotplot scale represents "mean expression in groups", and the circles represent "fraction of cells in group (%)".

competence, such as TGFB1, EGFR, and IGF2BP1/2/3, were identified (Figure S3H; Table S4D).

Process robustness following optimization is demonstrated through analytical assessment of the product's quality, safety, and purity

After confirming that process optimization did not compromise OSC identity or purity, two additional CG-OSC-L lots were produced to demonstrate process robustness. Analytical development was performed to define critical attributes required to assess potency and safety and ensure alignment with the QTPP (Table S1). In addition to standard attributes expected for IVF products (sterility, endotoxin, embryotoxicity), safety testing for OSCs must include additional testing to address risks associated with hiPSCs, including residual hiPSC presence, detection of communicable diseases, and screening for disease-related agents. Under controlled conditions, two additional OSC lots (#180 and #182) were manufactured, and analytical testing results demonstrated the reproducible and consistent outcomes (Table 1). The CG-OSC-L lots were also tested for mycoplasma, endotoxin, sterility, and human adventitious agents to ensure the safety of the clinical product (Table 2).

To assess the potency for *Fertilo* release, MOMA was developed to mimic clinical application using a surrogate species (mice). In this assay, fresh immature oocytes from hybrid B6/CBA mice at the germinal vesicle (GV) stage were collected from minimally stimulated female mice between 6 and 8 weeks of age. The immature oocytes were then subjected to IVM with IVM media alone (media-only control) or in the presence of different types of cells, including OSCs. Following IVM, the mature oocytes were fertilized via intracytoplasmic sperm injection (ICSI). After 5 days, the BFR was assessed to measure potency (Figure 4A).

Three negative control conditions were included: media-only control, media with non-viable (heat-inactivated) CG-OSCs, and media with mouse embryonic fibroblasts. The BFRs were consistent among these conditions (59%, 58%, and 61%, respectively), indicating that the improvement in BFR with OSC-IVM is a result of the specific activity of viable OSCs (Figure 4B). To evaluate the impact of the dose on OSC-IVM efficacy, in one condition, half of the recommended number of OSCs (50,000 OSCs per 100 μL) was added during IVM

Please cite this article in press as: Paulsen et al., Development of human induced pluripotent stem cell-derived ovarian support cells as a clinical-grade product for *in vitro* fertilization, Cell Stem Cell (2025), https://doi.org/10.1016/j.stem.2025.12.020

Table 2. Safety testing panel

Test	Specification	CG-hiPSC MCB	CG-OSC production lots	CG-OSC product	CG-OSC product 6 months storage	CG-OSC product 12 months storage
Genomic integrity	no karyotypic abnormalities detected	pass	NT	pass	pass	pass
Endotoxin	≤0.1 EU/mL	pass	pass	pass	NT	NT
Mycoplasma	not detected	pass	pass	pass	NT	NT
Sterility	no growth	pass	pass	pass	pass	pass
Adventitious agents (human test panel)	not detected	Pass	pass	pass	NT	NT
Adventitious agents (*in vivo*)	negative	pass	NT	NT	NT	NT
Adventitious agents (*in vitro*)	negative	pass	NT	NT	NT	NT
Adventitious agents (species- specific)	negative	pass	NT	NT	NT	NT
Retroviral contamination	negative	pass	NT	NT	NT	NT
Residual hiPSC—RT-qPCR	OCT4 ≤ 0.1%; NANOG ≤ 0.1%	NT	NT	pass	NT	NT
Residual doxycycline	≤0.06 μg/mL	NT	NT	pass	NT	NT
Mouse embryo assay—embryotoxicity	blastocyst formation ≥ 80%	NT	NT	pass	pass	pass

NT, not tested.

co-culture. In this condition, there was approximately half the improvement in day 5 BFR, compared with the full dose, indicating a dose-responsive relationship between OSC number and BFR (Figure 4B). To confirm the robustness of the process, the potency of OSCs derived from different genetic backgrounds (RUO-hiPSC and CG-hiPSC) was evaluated, and all lots exhibited an increased BFR, compared with controls, with the highest BFRs seen with CG-OSC lots (Figure 4B).

Clinical readiness of CG-OSC-L batches for OSC-IVM application

To facilitate translatability, the CG-hiPSC seed bank, generated under controlled conditions, was expanded into a master cell bank (MCB) under GMP-compliant manufacturing practices. As part of this transition, aseptic process simulation (APS) runs were conducted to validate sterility, assess contamination risks, and confirm the robustness of the manufacturing process before full-scale GMP production. A comprehensive risk assessment was performed on all materials and process steps involved in CG-hiPSC to CG-OSC manufacturing. Based on identified risks inherent to the process, targeted analytical tests were conducted to ensure safety and process control (Tables 1 and 2). Following CG-hiPSC expansion under GMP conditions, all testing met the predefined acceptance criteria, confirming the safety and suitability of the starting material (Tables 1 and 2). These results demonstrate that the manufacturing process is adequately controlled to enable GMP production of OSCs and the release of GMP *Fertilo* batches for application.

To evaluate the stability of the *Fertilo* final product, a long-term stability study was conducted to monitor key quality attributes, including OSC marker expression (identity), cell count and viability (conformance), potency, and safety, over a 12-month period. The 6- and 12-month stability under defined storage conditions demonstrated consistent product quality over time (Tables 1 and 2). In addition, the shipping stability study demonstrated that product quality, potency, and safety are maintained during a 7-day shipment period (Table 1). In-use stability testing showed that under the handling conditions specified in the instructions for use (IFU), *Fertilo* maintains its quality and potency attributes (Table 1). Overall, these stability studies establish the product shelf life and ensure that *Fertilo* remains safe and efficacious upon distribution and during use.

Application of CG-OSCs significantly improves IVM outcomes

To evaluate the clinical outcomes of *Fertilo* in humans, a first-in-human observational, longitudinal, cohort study was performed; this study enabled investigation of the safety and efficacy of *Fertilo* application. This study was performed in two phases; the first phase consisted of a multi-center, single arm observational evaluation in 20 patients with the primary purpose of safety evaluation and the establishment of clinical success metrics. The second phase of the evaluation was expanded to a limited comparator-controlled cohort comparison of twenty patents with 1:1 randomization between the two arms to provide measures of efficacy and inform future registrational clinical trial designs. The patients in both studies were premenopausal women between the ages of 18 and 37, who were appropriate candidates for IVF with normal ovarian reserve, as indicated by an

Please cite this article in press as: Paulsen et al., Development of human induced pluripotent stem cell-derived ovarian support cells as a clinical-grade product for *in vitro* fertilization, Cell Stem Cell (2025), https://doi.org/10.1016/j.stem.2025.12.020

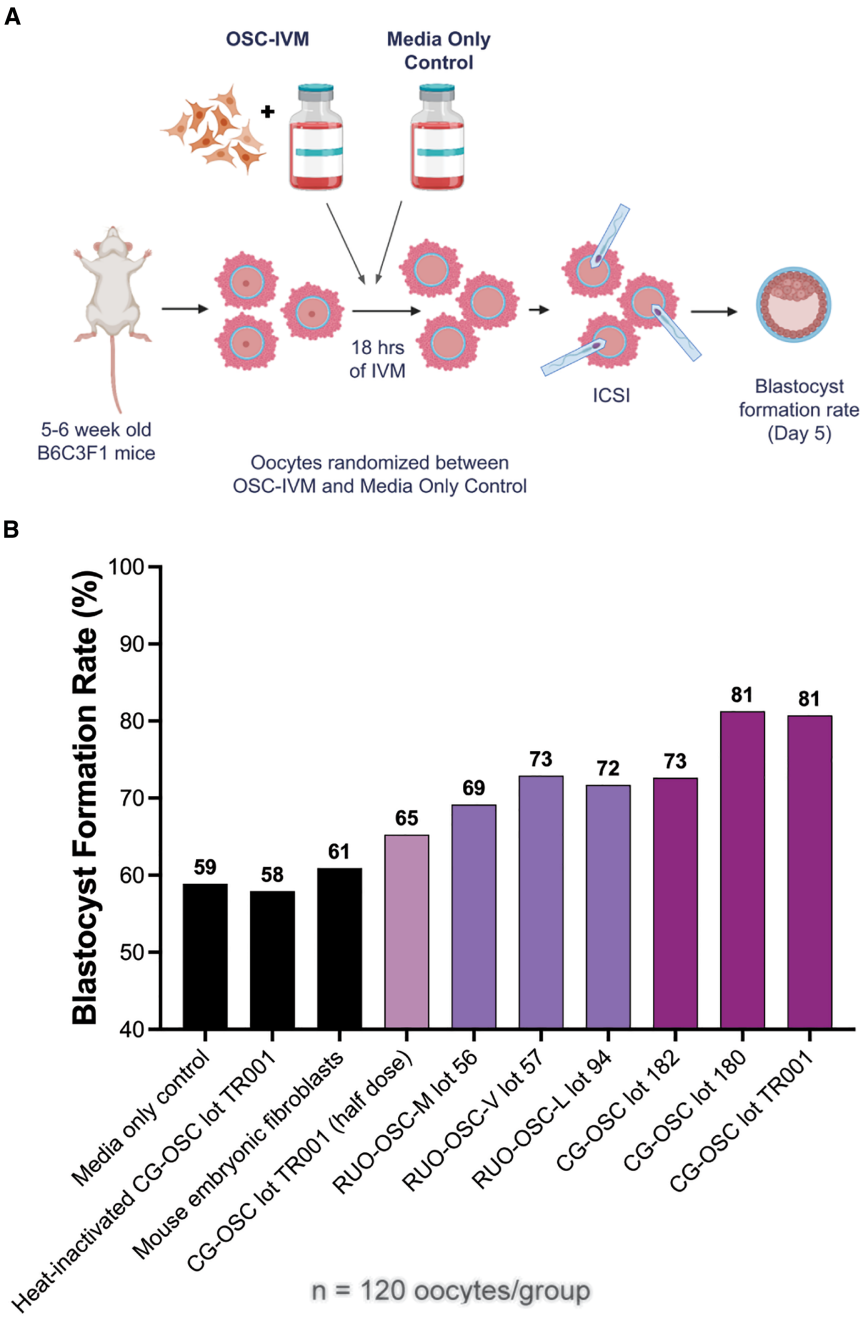

Figure 4. Establishment of MOMA for release of the clinical OSC-IVM product

(A) Schematic of the MOMA study design for OSC-IVM product release.

(B) BFR following OSC-IVM in various test conditions. The first three conditions represented by the black bars are the negative controls with no cells, inactivated cells, and alternative cells, respectively. The fourth condition is CG-OSCs with half the recommended amount of OSCs for OSC-IVM. Conditions five through seven represent OSC-IVM with RUO-OSCs, and the last three conditions represent OSC-IVM with CG-OSCs. A total of 120 oocytes were evaluated in each condition (n = 120).

anti-mullerian hormone (AMH) of greater than 2 ng/mL, and primary infertility. Additional details about the inclusion and exclusion criteria for patients are provided in the STAR Methods section. Information about patient demographics and treatment conditions (Table S9), as well as the workflow of both phases of the study (Figure S4), are provided in the supplemental information.

In phase 1, 20 infertile patients were recruited. Following minimal stimulation cycles, immature cumulus-oocyte complexes (COCs) were collected from patients, subjected to IVM with *Fertilo*, and key embryological and clinical outcomes were assessed. The results for each outcome were determined based on the number of samples that proceeded to each step. The MII maturation rate was 68% per COC retrieved based on the presence of a first polar body (PB1) (Figure 5A). Between 16 and 18 h post-ICSI, the fertilization rate was determined to be 84% per mature MII based on the formation of two pronuclei (Figure 5A). The cleavage rate was determined at 3 days post-ICSI based on the presence of 2 or more cells, and the total and high-quality (HQ) BFRs were determined on days 5–7 post-ICSI, based on cavitation and a 3BB or greater score based on the Gardner scale, respectively. The cleavage rate was 91%, the BFR was 42%, and the HQ BFR was 38% (Figure 5A); these percentages were calculated per fertilized embryo. The euploidy rate, which was determined within 7 days post-ICSI via PGT-A analysis, was 64% per blastocyst biopsy (Figure 5A). Finally, the biochemical (implantation) and clinical pregnancy rate were determined per embryo transfer. Biochemical pregnancy was assessed at days 10–14 post transfer based on a β-human chorionic gonadotropin (hCG) > 5 mIU/mL; the rate of successful implantation was 60% (Figure 5A). Ongoing clinical pregnancy was assessed at a minimum of 10 weeks post-embryo transfer based on the presence of a visible gestational sac with a fetal heartbeat via ultrasound at 10–12 weeks' gestation; the rate of ongoing clinical pregnancy per embryo transfer was 53% (Figure 5A). Notably, the first live birth of a healthy singleton female following an OSC-IVM cycle with *Fertilo* occurred at 38.5 weeks. At birth, the baby was 3,255 g, 49.5 cm, and scored a 9/9 on the Apgar scale, demonstrating no congenital abnormalities after a vaginal birth. Since then, there have been five additional healthy live births in this study, with additional pregnancies ongoing.

After verifying the safety and initial efficacy of *Fertilo* with a minimal stimulation regimen, an expansion of this study was

Please cite this article in press as: Paulsen et al., Development of human induced pluripotent stem cell-derived ovarian support cells as a clinical-grade product for *in vitro* fertilization, Cell Stem Cell (2025), https://doi.org/10.1016/j.stem.2025.12.020

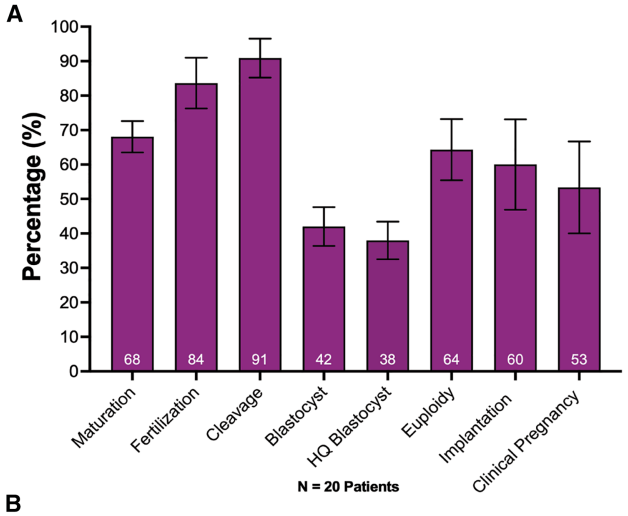

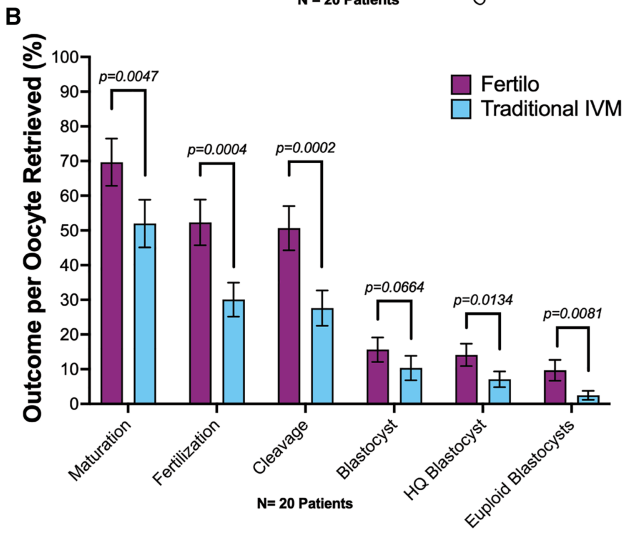

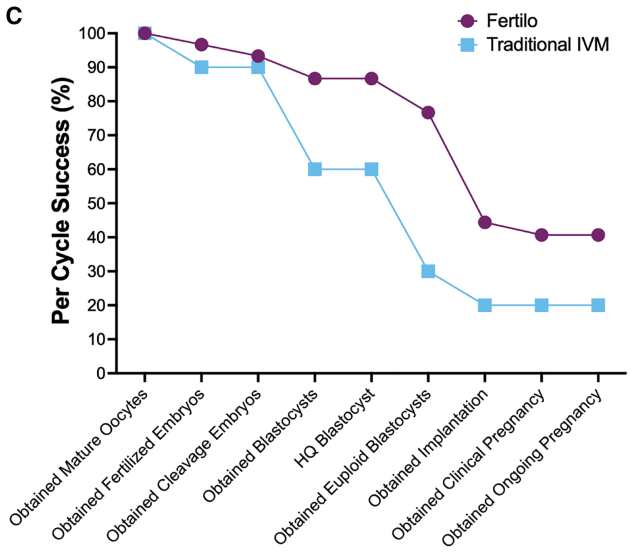

Figure 5. Clinical application of CG-OSCs significantly improves IVM outcomes

(A) Clinical outcomes of a single arm, multi-site observational evaluation following OSC co-culture for IVM. The percentages for outcomes were determined incrementally based on the number of samples that proceeded each step. Data are presented as the mean ± SEM.

(B) Comparative evaluation of clinical outcomes following IVM co-culture with OSCs (*Fertilo*) vs. IVM culture in media alone (traditional IVM). The outcomes were assessed based on the initial number of oocytes retrieved. The comparative statistical analysis between traditional IVM and *Fertilo* groups for embryological outcomes was performed using logistic regression. Significance was based on the *Fertilo* distribution, compared with the traditional IVM mean, for each development point. A p value of less than 0.05 was considered statistically significant in all tests. Data are presented as the mean ± SEM, with 10 patients included in each group (N = 20 total patients).

(C) Compiled results from both clinical evaluations per treatment cycle. Data show the percentage of treatment cycles that lead to successful completion of each outcome.

initiated. In the second phase, a limited comparator-controlled cohort evaluation of *Fertilo* vs. traditional IVM (monophasic IVM medium) was performed in 20 infertile patients (10 per treatment arm). The efficacy of *Fertilo* was compared with that of traditional IVM based on embryological endpoints, assessed based on the percentage of samples that achieved each outcome per COC retrieved (Figure 5B). Following IVM, the MII oocyte maturation rate was determined; the MII maturation rate of the *Fertilo* group was significantly greater than that of the traditional IVM group (70% ± 7% vs. 52% ± 7%, p = 0.0047; Figure 5B). MII oocytes were then fertilized via ICSI, and the fertilization rate per COC was significantly higher in the *Fertilo* group than in the traditional IVM group (52% ± 7% vs. 30% ± 5%, p = 0.0004; Figure 5B). On day 3 post-ICSI, the percentage cleavage in the *Fertilo* group was significantly higher than that in the traditional IVM group (51% ± 6% vs. 28% ± 5%, p = 0.0002; Figure 5B). The overall blastocyst, HQ blastocyst, and euploid BFRs were determined within 7 days post-ICSI. The rate of blastocyst formation in the *Fertilo* group was slightly but not significantly higher than that in the traditional IVM group (16% ± 4% vs. 10% ± 4%, p = 0.0664; Figure 5B). However, when considering only HQ blastocysts, defined as those of freezable quality with a score of 3BB or greater based on the Gardner scale, the *Fertilo* group had a significantly higher HQ BFR than the traditional IVM group (14% ± 3% vs. 7% ± 2%, p = 0.0134; Figure 5B). Finally, the euploid BFR of the *Fertilo* group, based on PGT-A analysis, was significantly greater than that of the traditional IVM group (10% ± 3% vs. 2% ± 1%, p = 0.0081; Figure 5B). Notably, 8 of 10 patients in the *Fertilo* group vs. only 3 of 10 patients in the traditional IVM group had at least 1 euploid blastocyst available for transfer. Of the eight patients in the *Fertilo* group, one became spontaneously pregnant naturally, one had an embryo transfer from alternative treatment, one is still awaiting embryo transfer, and five have undergone embryo transfer. There have been two healthy live births in this group, with one ongoing pregnancy awaiting delivery and two implantation failures. In the traditional IVM group, all three patients underwent embryo transfer, with two resulting in healthy live births and one implantation failure.

Collected data on adverse events up to this point are provided in the supplemental information (Table S9). Adverse events related to minimal stimulation were considered non-*Fertilo*

Please cite this article in press as: Paulsen et al., Development of human induced pluripotent stem cell-derived ovarian support cells as a clinical-grade product for *in vitro* fertilization, Cell Stem Cell (2025), https://doi.org/10.1016/j.stem.2025.12.020

related, as *Fertilo* application in all cases consisted of IVM after oocyte retrieval. The compiled data of both phases of the study based on successful outcomes per cycle demonstrated that OSC-IVM (*Fertilo*, 41%) has a better treatment success rate than traditional IVM (20%) (Figure 5C); the success rate of treatment is based on the rate of ongoing pregnancy, defined as a fetal sac visualized with ultrasound with detectable fetal heart rate at weeks 10–12 of gestation. In addition, although the blastocyst and euploid blastocyst rates were the most similar in the outcome comparison per COC, comparison of these rates per cycle shows that *Fertilo* led to substantially more successful blastocyst and euploid blastocyst formation per cycle than traditional IVM (blastocyst 86.7% vs. 60%; euploid blastocyst 77% vs. 30%) (Figure 7C). The data for both phases combined, calculated per COC and stage, further confirm the improvement in outcomes with *Fertilo* (Table S8).

DISCUSSION

Oocyte maturation *in vivo* relies on extensive crosstalk between the developing oocytes and somatic ovarian cells, including granulosa and theca cells.[21,32,33] This crosstalk is notably absent in traditional IVM, potentially contributing to incomplete or low rates of oocyte maturation.[34,35] While IVM culture with granulosa cells can improve IVM outcomes,[15,16] the broad clinical utilization of primary granulosa cells is not feasible. To address these concerns, we recently demonstrated that supplementing traditional IVM media with hiPSC-derived OSCs leads to higher oocyte maturation and euploid embryo formation rates,[17] likely by restoring key signaling pathways and recapitulating the physiological ovarian environment.

Here, we describe the process development and clinical application of *Fertilo*, an hiPSC-derived OSC product. The OSC manufacturing process was optimized by using the highest-quality raw materials while preserving cellular identity and function. Multiple clinical OSC lots were produced using the optimized process, analytically characterized, and assessed for potency using MOMA. After the clinical OSC lots were determined fit for release, *Fertilo* was evaluated clinically via OSC-IVM in a two-phase study comprising an observational safety phase and a comparative control phase. Clinical application of *Fertilo* improved oocyte maturation, embryological outcomes, and pregnancy rates, with no *Fertilo*-related adverse events.

First, OSC generation was achieved using TF-directed hiPSC differentiation via overexpression of *NR5A1*, *RUNX2*, and *GATA4*. Co-culture of human oocytes with RUO-OSCs yielded an approximately 65% maturation rate, similar to the percentage of mature oocytes collected following conventional stimulation protocols, which typically ranges between 70% and 90%.[36–39] NGS analyses of *Fertilo*-treated oocytes and subsequently derived embryos detected no residual OSC genetic material, indicating minimal risk of carryover or *in vivo* transfer alongside embryos. As proteins and metabolites exhibit lower intrinsic stability and are therefore regarded as less critical to the long-term safety of the developing embryo, as evidenced by the persistence of stable maternal proteins during the oocyte-to-embryo transition,[40] we consider genomic analysis to be sufficient to demonstrate the lack of carryover risk.

Raw material optimization not only reduces the risk of adventitious agents or toxins in the final product but also increases lot-to-lot reproducibility. To enable clinical translation, several raw materials were substituted with higher-quality alternatives, including the differentiation substrate and hiPSC starting material. While both vitronectin and laminin supported successful differentiation, laminin yielded higher cell viability and an improved OSC:hiPSC ratio, making it the preferred substrate. Subsequently, a donor hiPSC line was engineered using the same strategy as the RUO-hiPSC line.[8] Nine candidate clones were evaluated, with clone 2-D10 selected as the most suitable. Notably, despite raw material substitutions and the utilization of the CG-hiPSC line, TF-directed differentiation consistently generated functional OSCs.

Implementation of higher-quality raw materials further improved batch consistency and increased the proportion of target GCs, expressing markers such as *MDK*, *CDH2*, and *ITGB1*. scRNA-seq results demonstrated strong expression of *MDK* across OSC clusters, as well as high expression of *BMP*, *CYP19A*, and *EGFR*, indicating a predominantly mural GC identity.[18,41–43] This result is consistent with prior data showing significantly upregulated expression of *CYP19A1*—which is essential for estrogen biosynthesis—in response to FSH challenge, a hallmark of mural granulosa cell biology.[18]

The hypothesis of a paracrine mechanism of action is based not only on the expression of growth factors and ligand-receptor genes but also of proteins identified in the conditioned media of OSCs, including *TGFB1*, *EGFR*, and *IGFBP1/2/3*, which are associated with oocyte maturation and developmental competence (Table S5).[31,44–47] In addition, previous studies demonstrated that not only are oocytes modulated by OSCs, but the OSC molecular signature is also modulated by oocytes.[18] These findings are also supported by previous transcriptomic analysis showing human oocytes matured with *Fertilo* exhibited enrichment in pathways related to translation, oocyte maturation, and embryonic development, similar to *in vivo* matured oocytes[18]; this enrichment was absent in oocytes matured via traditional IVM, which instead showed enrichment in markers associated with DNA damage and the cell cycle, implying potential stalling of meiotic progression.[18] Therefore, MII oocytes matured via OSC-IVM may exhibit a higher developmental competence than those matured via traditional IVM.

A key consideration for clinical development is process consistency; therefore, analytical methods were developed to assess product potency, identity, purity, and safety, ensuring alignment with criteria in the QTPP. To ensure product purity, flow cytometry analysis of OSC markers and RT-qPCR analysis of pluripotency markers were utilized for analytical assessment. These methods were selected because they provide quantitative, reproducible, and objective measurements that can be readily standardized, qualified, and validated. The purity of the population of OSCs in *Fertilo* is determined based on the expression of *CD82* and *FOXL2*, determined via flow cytometry, and RT-qPCR analysis of the pluripotent markers *POU5F1* (OCT4) and *NANOG*. As part of our validation of analytical procedures, we demonstrated that the RT-qPCR method is sufficient to detect 0.01% hiPSCs in the cell population. Overall, the results demonstrated that the release criteria were consistently met across multiple lots.

Please cite this article in press as: Paulsen et al., Development of human induced pluripotent stem cell-derived ovarian support cells as a clinical-grade product for *in vitro* fertilization, Cell Stem Cell (2025), https://doi.org/10.1016/j.stem.2025.12.020

A novel potency assay, referred to as MOMA, was developed specifically to evaluate the efficacy of different lots of *Fertilo*. This assay evaluates oocyte maturation followed by embryo formation in a surrogate species (mice)[20] to provide information about the therapeutic activity of hiPSC-derived OSCs. MOMA results showed that OSC-IVM improved the BFR of murine oocytes, compared with all negative conditions, demonstrating that this assay is a suitable strategy for OSC batch release.

To ensure the clinical readiness of *Fertilo*, the CG-hiPSC seed bank was expanded into a GMP-compliant MCB, with comprehensive risk assessment, release testing, and stability studies confirming manufacturing robustness. Following establishment of the clinically suitable product, *Fertilo* was evaluated in a two-phase longitudinal cohort analysis: phase 1 consisted of a single arm multi-center observational safety study, and phase 2 consisted of an expanded comparative evaluation against traditional IVM. Importantly, the only difference between traditional IVM and an IVM protocol with *Fertilo* is the addition of OSCs to the culture dish during IVM and additional washing steps to ensure that any residual product is removed.

To date, *Fertilo* has resulted in 11 ongoing pregnancies with 8 healthy live births and additional births scheduled for delivery, compared with 2 ongoing pregnancies and 2 live births with traditional IVM. The successful clinical pregnancy outcomes and multiple healthy live births establish the efficacy and favorable safety profile of *Fertilo*. *Fertilo* significantly improved the MII maturation and euploid BFRs, compared with traditional IVM, translating into a higher proportion of patients reaching embryo transfer (8 of 10 patients in the *Fertilo* group vs. 3 of 10 patients in the traditional IVM group). Compiled data from both phases revealed that overall treatment success, defined as ongoing pregnancy per cycle, was 41% with *Fertilo* vs. 20% with traditional IVM. Previous clinical studies of traditional IVM show ongoing pregnancy rates of approximately 25% per cycle, further confirming that the rate of ongoing pregnancy with *Fertilo* is greater than that seen with traditional IVM.[12,13] Although the current clinical data do not indicate a significant improvement in BFR, there was a significant increase in the HQ BFR. Given that a major drawback of IVM is that embryos are often of low quality and have low developmental competence, we consider the significant increase in HQ blastocyst formation with *Fertilo* to be the more meaningful outcome. In both phases, safety and efficacy analyses of fetal development and maternal health remain ongoing, with only minor adverse events reported in either phase (Table S9).

Notably, *Fertilo* is the first hiPSC-derived product to receive investigational new drug (IND) clearance for a phase 3 clinical trial in the US. This phase 3 study of 500 participants will include approximately 250 patients treated with *Fertilo*, with comprehensive safety and efficacy monitoring planned throughout the study. In addition, robust post-trial surveillance has been implemented, including a structured follow-up registry to monitor patients longitudinally. These measures ensure continued assessment of both safety and efficacy, reinforcing *Fertilo*'s favorable safety profile and supporting its responsible global clinical use.

In summary, *Fertilo* represents the first clinical application of an hiPSC-derived product in women's health. By improving the maturation and reproductive outcomes following minimal stimulation, OSC-IVM increases the likelihood of successful IVF cycles for patients who are at a high risk of OHSS. Although *Fertilo* is particularly suited for IVM, its application can also be beneficial for rescue IVM, which is performed if a controlled ovarian stimulation (COS) cycle has not yielded many mature oocytes; however, this application is limited as COS protocols typically yield most mature oocytes. More broadly, the application of *Fertilo* is beneficial for the wider population of women undergoing ART as minimal stimulation reduces the side effects, cost, and length of stimulation cycles.

Beyond ART, OSCs could have potential uses in patients with medical conditions that limit the use of hormonal stimulation, such as autoimmune diseases or estrogen-sensitive disorders. Additionally, *Fertilo* may provide new fertility preservation strategies for patients undergoing gonadotoxic treatments or for oncofertility patients, for whom the duration of each cycle is critical. Future studies should explore these applications further to expand the clinical scope of this platform.

Limitations of the study

This study represents a significant advancement in women's health through the clinical development of an hiPSC-derived OSC product; however, further studies will be needed to fully define the mechanism of action. While gene expression and proteomics analyses support a paracrine mechanism involving OSC-oocyte crosstalk, the complexity of the ovarian environment and the limited availability of human samples, particularly with the consideration of generating human embryos without intended implantation, constrain deeper mechanistic investigation. Given these limitations and the complex and dynamic nature of *Fertilo*'s activity, we consider the presented genomic and proteomic data sufficient to support a paracrine mechanism of action within the scope of this clinical application-focused study.

Additional data will be needed to further assess the efficacy of *Fertilo* clinically across broader patient populations. As a first-in-human evaluation of *Fertilo*, enrollment in this study was limited to a narrowly defined population; nevertheless, the results demonstrate clinical feasibility and successful outcomes. Ongoing clinical monitoring will provide additional evaluation of pregnancy outcomes. To date, *Fertilo* has resulted in 8 healthy live births, with 3 additional ongoing pregnancies and additional transfers pending; these numbers are expected to grow as additional patients are enrolled in planned clinical studies.

RESOURCE AVAILABILITY

Lead contact

Requests for further information and resources should be directed to and will be fulfilled by the lead contact, Christian C. Kramme (christian@gametogen.com).

Materials availability

All unique material generated in this study will be available from the lead contact with a completed materials transfer agreement.

Data and code availability

- Data: proteomics data have been deposited at GEO and are publicly available as of the date of publication. RNA-seq data have been deposited at GEO as GEO: GSE313528 and are publicly available as of the date of publication. All remaining data reported in this paper will be

shared by the lead contact upon request. For clinical data, appropriate anonymized data will be made available upon valid request.
- Code: this paper does not report original code.
- Additional information: any additional information required to reanalyze the data reported in this paper is available from the lead contact upon request.

ACKNOWLEDGMENTS

This work was performed with the support of clinical partnerships at Spring Fertility New York, Extend Fertility, Ruber Clinic of Madrid, Tambre Clinic of Madrid, Pranor Clinic of Lima, and Fertilidad Integral of Mexico City. We are thankful for the dedicated support and work of the embryology and support staff teams at these clinics in coordinating and managing the collaborative study, as well as the technical support of Kathy Potts, Graham Rockwell, Alexa Giovannini, Christopher Collado, and Karina Flores. We additionally thank the Wyss Institute for Biologically Inspired Engineering at Harvard University for material transfer of reagents used in the preclinical sections of this work. We thank Professor Mary Herbert, Professor Phillip Jordan, Professor George Church, Professor Kristin Baldwin, Professor Pranam Chatterjee, Klaus Wiemer, Dr. Jamie Knopman, and Dr. Sara Vaughn for advice and guidance on the use of OSCs in IVM work. We also thank the New York University flow cytometry and imaging cores, the Proteomics and Metabolomics Core Facility at Weill Cornell Medicine, Embryotools of Barcelona, and Azenta/Genewiz for their assistance in data generation and analysis. This work was funded by the for-profit biotechnology company Gameto Inc.

AUTHOR CONTRIBUTIONS

C.C.K., B.P., F.B., A.D.N., and S.P. conceived the experiments. S.P., M.M., I.G.G., E.M.M., E.I.L., P.R., C.C., J.M., W.M., P.P., and L.G. performed all embryology work for the study; C.C.K. supervised their work. B.P., M.J., A.B.F., A.D.N., and F.B. produced and qualified OSC batches; C.C.K. supervised their work. B.P. and S.K. performed bulk- and scRNA-seq analysis and cell-type assignments. F.B. performed proteomic experiments and analysis as well as development of the MOMA assay. A.B.F. coordinated the assay logistics and quality process development. C.R., E.N., A.E., L.N.-P., J.G., E.M., and P.V. performed oocyte retrievals and patient treatments. D.R., G.H., P.B., M.D.V., D.F.A, L.G., P.V., E.M., J.G., and C.C.K. developed and refined clinical treatment protocols and study design and reviewed clinical safety and efficacy outcomes as part of the safety monitoring board; C.C.K., B.P., F.B., and C.L. wrote the manuscript with significant input from all authors.

DECLARATION OF INTERESTS

B.P., F.B., A.D.N., M.J., S.K., S.P., M.M., A.B.F., C.L., P.B., and C.C.K. are/were employees and shareholders of the for-profit biotechnology company Gameto Inc. while performing this work. D.F.A., M.D.V., and P.B. are members of the advisory board for the for-profit biotechnology company Gameto Inc. C.C.K., S.P., M.M., B.P., and A.D.N. are listed on a patent covering the use of OSCs for IVM: U.S. Provisional Patent Application No. 63/492,210. Additionally, C.C.K. is listed on three patents covering the use of OSCs for IVM: U.S. Patent Application No. 17/846,725; U.S Patent Application No. 17/846,845; and International Patent Application No. PCT/US2023/026012. C.C.K. is listed on three patents for the TF-directed differentiation of granulosa-like cells from stem cells: International Patent Application No. PCT/US2023/065140; U.S. Provisional Application No. 63/326,640; and U.S. Provisional Application No. 63/444,108.

STAR★METHODS

Detailed methods are provided in the online version of this paper and include the following:

SUPPLEMENTAL INFORMATION

Supplemental information can be found online at https://doi.org/10.1016/j.stem.2025.12.020.

Received: July 23, 2025
Revised: October 30, 2025
Accepted: December 18, 2025

REFERENCES

1. Cox, C.M., Thoma, M.E., Tchangalova, N., Mburu, G., Bornstein, M.J., Johnson, C.L., and Kiarie, J. (2022). Infertility prevalence and the methods of estimation from 1990 to 2021: a systematic review and meta-analysis. Hum. Reprod. Open *2022*, hoac051. https://doi.org/10.1093/hropen/hoac051.
2. Moradi, Y., Shams-Beyranvand, M., Khateri, S., Gharahjeh, S., Tehrani, S., Varse, F., Tiyuri, A., and Najmi, Z. (2021). A systematic review on the prevalence of endometriosis in women. Indian J. Med. Res. *154*, 446–454. https://doi.org/10.4103/ijmr.IJMR_817_18.
3. Shrivastava, S., and Conigliaro, R.L. (2023). Polycystic Ovarian Syndrome. Med. Clin. North Am. *107*, 227–234. https://doi.org/10.1016/j.mcna.2022.10.004.
4. Ballard, K.D., Seaman, H.E., de Vries, C.S., and Wright, J.T. (2008). Can symptomatology help in the diagnosis of endometriosis? Findings from a national case-control study–Part 1. BJOG *115*, 1382–1391. https://doi.org/10.1111/j.1471-0528.2008.01878.x.
5. Mercuri, N.D., and Cox, B.J. (2022). The need for more research into reproductive health and disease. eLife *11*, e75061. https://doi.org/10.7554/eLife.75061.
6. Smith, K. (2023). Women's health research lacks funding – in a series of charts. Nature *617*, 28–29. https://doi.org/10.1038/d41586-023-01475-2.
7. Lipskind, S., Lindsey, J.S., Gerami-Naini, B., Eaton, J.L., O'Connell, D., Kiezun, A., Ho, J.W.K., Ng, N., Parasar, P., Ng, M., et al. (2018). An Embryonic and Induced Pluripotent Stem Cell Model for Ovarian Granulosa Cell Development and Steroidogenesis. Reprod. Sci. *25*, 712–726. https://doi.org/10.1177/1933719117725814.
8. Pierson Smela, M.D., Kramme, C.C., Fortuna, P.R.J., Adams, J.L., Su, R., Dong, E., Kobayashi, M., Brixi, G., Kavirayuni, V.S., Tysinger, E., et al. (2023). Directed differentiation of human iPSCs to functional ovarian granulosa-like cells via transcription factor overexpression. eLife *12*, e83291. https://doi.org/10.7554/eLife.83291.

9. Wu, G.M.J., Chen, A.C.H., Yeung, W.S.B., and Lee, Y.L. (2023). Current progress on in vitro differentiation of ovarian follicles from pluripotent stem cells. Front. Cell Dev. Biol. *11*, 1166351. https://doi.org/10.3389/fcell.2023.1166351.

10. Jung, D., Xiong, J., Ye, M., Qin, X., Li, L., Cheng, S., Luo, M., Peng, J., Dong, J., Tang, F., et al. (2017). In vitro differentiation of human embryonic stem cells into ovarian follicle-like cells. Nat. Commun. *8*, 15680. https://doi.org/10.1038/ncomms15680.

11. Marchante, M., Barrachina, F., Piechota, S., Fernandez-González, M., Giovannini, A., Smith, T., Kats, S., Paulsen, B., González, E., Calvente, V., et al. (2024). Donor side effects experienced under minimal controlled ovarian stimulation with in vitro maturation vs. conventional controlled ovarian stimulation for in vitro fertilization treatment. F. S. Sci. *5*, 242–251. https://doi.org/10.1016/j.xfss.2024.05.002.

12. Ortega-Hrepich, C., Stoop, D., Guzmán, L., Van Landuyt, L., Tournaye, H., Smitz, J., and De Vos, M. (2013). A "freeze-all" embryo strategy after in vitro maturation: a novel approach in women with polycystic ovary syndrome? Fertil. Steril. *100*, 1002–1007. https://doi.org/10.1016/j.fertnstert.2013.06.018.

13. Zheng, X., Guo, W., Zeng, L., Zheng, D., Yang, S., Xu, Y., Wang, L., Wang, R., Mol, B.W., Li, R., et al. (2022). In vitro maturation without gonadotropins versus in vitro fertilization with hyperstimulation in women with polycystic ovary syndrome: a non-inferiority randomized controlled trial. Hum. Reprod. *37*, 242–253. https://doi.org/10.1093/humrep/deab243.

14. Vuong, L.N., Pham, T.D., Ho, T.M., and De Vos, M. (2023). Outcomes of clinical in vitro maturation programs for treating infertility in hyper responders: a systematic review. Fertil. Steril. *119*, 540–549. https://doi.org/10.1016/j.fertnstert.2023.01.046.

15. Jahromi, B.N., Mosallanezhad, Z., Matloob, N., Davari, M., and Ghobadifar, M.A. (2015). The potential role of granulosa cells in the maturation rate of immature human oocytes and embryo development: A co-culture study. Clin. Exp. Reprod. Med. *42*, 111–117. https://doi.org/10.5653/cerm.2015.42.3.111.

16. Johnson, J.E., Higdon, H.L., 3rd, and Boone, W.R. (2008). Effect of human granulosa cell co-culture using standard culture media on the maturation and fertilization potential of immature human oocytes. Fertil. Steril. *90*, 1674–1679. https://doi.org/10.1016/j.fertnstert.2007.06.017.

17. Piechota, S., Marchante, M., Giovannini, A., Paulsen, B., Potts, K.S., Rockwell, G., Aschenberger, C., Noblett, A.D., Figueroa, A.B., Sanchez, M., et al. (2023). Human-induced pluripotent stem cell-derived ovarian support cell co-culture improves oocyte maturation in vitro after abbreviated gonadotropin stimulation. Hum. Reprod. *38*, 2456–2469. https://doi.org/10.1093/humrep/dead205.

18. Paulsen, B., Piechota, S., Barrachina, F., Giovannini, A., Kats, S., Potts, K.S., Rockwell, G., Marchante, M., Estevez, S.L., Noblett, A.D., et al. (2024). Rescue in vitro maturation using ovarian support cells of human oocytes from conventional stimulation cycles yields oocytes with improved nuclear maturation and transcriptomic resemblance to in vivo matured oocytes. J. Assist. Reprod. Genet. *41*, 2021–2036. https://doi.org/10.1007/s10815-024-03143-4.

19. Sanchez, F., Le, A.H., Ho, V.N.A., Romero, S., Van Ranst, H., De Vos, M., Gilchrist, R.B., Ho, T.M., Vuong, L.N., and Smitz, J. (2019). Biphasic in vitro maturation (CAPA-IVM) specifically improves the developmental capacity of oocytes from small antral follicles. J. Assist. Reprod. Genet. *36*, 2135–2144. https://doi.org/10.1007/s10815-019-01551-5.

20. Marchante, M., Barrachina, F., Mestres, E., Acacio, M., Potts, K.S., Piechota, S., Paulsen, B., Noblett, A.D., Figueroa, A.B., Costa-Borges, N., et al. (2024). Ovarian support cell in vitro maturation (OSC-IVM) results in healthy murine live births with no evidence of reprotoxicology in a multi-generational study. Reprod. Biomed. Online *50*, 104695.

21. Zhang, Y., Yan, Z., Qin, Q., Nisenblat, V., Chang, H.-M., Yu, Y., Wang, T., Lu, C., Yang, M., Yang, S., et al. (2018). Transcriptome Landscape of Human Folliculogenesis Reveals Oocyte and Granulosa Cell Interactions. Mol. Cell *72*, 1021–1034.e4. https://doi.org/10.1016/j.molcel.2018.10.029.

22. Kramme, C., Plesa, A.M., Wang, H.H., Wolf, B., Smela, M.P., Guo, X., Kohman, R.E., Chatterjee, P., and Church, G.M. (2021). An integrated pipeline for mammalian genetic screening. Cell Rep. Methods *1*, 100082. https://doi.org/10.1016/j.crmeth.2021.100082.

23. Garcia-Alonso, L., Lorenzi, V., Mazzeo, C.I., Alves-Lopes, J.P., Roberts, K., Sancho-Serra, C., Engelbert, J., Marečková, M., Gruhn, W.H., Botting, R.A., et al. (2022). Single-cell roadmap of human gonadal development. Nature *607*, 540–547. https://doi.org/10.1038/s41586-022-04918-4.

24. Ilicic, T., Kim, J.K., Kolodziejczyk, A.A., Bagger, F.O., McCarthy, D.J., Marioni, J.C., and Teichmann, S.A. (2016). Classification of low quality cells from single-cell RNA-seq data. Genome Biol. *17*, 29. https://doi.org/10.1186/s13059-016-0888-1.

25. Vanorny, D.A., and Mayo, K.E. (2017). The role of Notch signaling in the mammalian ovary. Reproduction *153*, R187–R204. https://doi.org/10.1530/REP-16-0689.

26. Goud, P.T., Goud, A.P., Qian, C., Laverge, H., Van der Elst, J., De Sutter, P., and Dhont, M. (1998). In-vitro maturation of human germinal vesicle stage oocytes: role of cumulus cells and epidermal growth factor in the culture medium. Hum. Reprod. *13*, 1638–1644. https://doi.org/10.1093/humrep/13.6.1638.

27. Richani, D., and Gilchrist, R.B. (2018). The epidermal growth factor network: role in oocyte growth, maturation and developmental competence. Hum. Reprod. Update *24*, 1–14. https://doi.org/10.1093/humupd/dmx029.

28. Amargant, F., Zhou, L.T., Yuan, Y., Nahar, A., Krisher, R.L., Spate, L.D., Roberts, R.M., Prather, R.S., Rowell, E.E., Laronda, M.M., et al. (2023). FGF2, LIF, and IGF1 (FLI) supplementation during human in vitro maturation enhances markers of gamete competence. Hum. Reprod. *38*, 1938–1951. https://doi.org/10.1093/humrep/dead162.

29. Ikeda, S., and Yamada, M. (2014). Midkine and cytoplasmic maturation of mammalian oocytes in the context of ovarian follicle physiology. Br. J. Pharmacol. *171*, 827–836. https://doi.org/10.1111/bph.12311.

30. Mu, H., Cai, S., Wang, X., Li, H., Zhang, L., Li, H., and Xiang, W. (2022). RNA binding protein IGF2BP1 meditates oxidative stress-induced granulosa cell dysfunction by regulating MDM2 mRNA stability in an m6A-dependent manner. Redox Biol. *57*, 102492. https://doi.org/10.1016/j.redox.2022.102492.

31. Xu, X., Shen, H.-R., Zhang, J.-R., and Li, X.-L. (2022). The role of insulin-like growth factor 2 mRNA binding proteins in female reproductive pathophysiology. Reprod. Biol. Endocrinol. *20*, 89. https://doi.org/10.1186/s12958-022-00960-z.

32. Zhang, H., Lu, S., Xu, R., Tang, Y., Liu, J., Li, C., Wei, J., Yao, R., Zhao, X., Wei, Q., et al. (2020). Mechanisms of estradiol-induced EGF-like factor expression and oocyte maturation via G protein-coupled estrogen receptor. Endocrinology *161*, bqaa190. https://doi.org/10.1210/endocr/bqaa190.

33. Shi, Y., Guo, Y., Zhou, J., Cui, G., Cheng, J.-C., Wu, Y., Zhao, Y.-L., Fang, L., Han, X., Yang, Y.-G., et al. (2023). A spatiotemporal gene expression and cell atlases of the developing rat ovary. Cell Prolif. *56*, e13516. https://doi.org/10.1111/cpr.13516.

34. Gong, X., Li, H., and Zhao, Y. (2022). The improvement and clinical application of human oocyte in vitro maturation (IVM). Reprod. Sci. *29*, 2127–2135. https://doi.org/10.1007/s43032-021-00613-3.

35. Das, M., and Son, W.-Y. (2023). In vitro maturation (IVM) of human immature oocytes: is it still relevant? Reprod. Biol. Endocrinol. *21*, 110. https://doi.org/10.1186/s12958-023-01162-x.

36. Lee, H.J., Jee, B.C., Suh, C.S., Kim, S.H., and Moon, S.Y. (2012). Oocyte maturity in relation to woman's age in in vitro fertilization cycles stimulated by single regimen. Yonsei Med. J. *53*, 181–185. https://doi.org/10.3349/ymj.2012.53.1.181.

37. Li, J., Shen, J., Zhang, X., Peng, Y., Zhang, Q., Hu, L., Reichetzeder, C., Zeng, S., Li, J., Tian, M., et al. (2022). Risk factors associated with preterm birth after IVF/ICSI. Sci. Rep. *12*, 7944. https://doi.org/10.1038/s41598-022-12149-w.

38. Magaton, I.M., Helmer, A., Eisenhut, M., Roumet, M., Stute, P., and von Wolff, M. (2023). Oocyte maturity, oocyte fertilization and cleavage-stage embryo morphology are better in natural compared with high-dose gonadotrophin stimulated IVF cycles. Reprod. Biomed. Online *46*, 705–712. https://doi.org/10.1016/j.rbmo.2022.11.008.

39. Capper, E., Krohn, M., Summers, K., Mejia, R., Sparks, A., and Van Voorhis, B.J. (2022). Low oocyte maturity ratio is associated with a reduced in vitro fertilization and intracytoplasmic sperm injection live birth rate. Fertil. Steril. *118*, 680–687. https://doi.org/10.1016/j.fertnstert.2022.07.008.

40. Zhang, H., Ji, S., Zhang, K., Chen, Y., Ming, J., Kong, F., Wang, L., Wang, S., Zou, Z., Xiong, Z., et al. (2023). Stable maternal proteins underlie distinct transcriptome, translatome, and proteome reprogramming during mouse oocyte-to-embryo transition. Genome Biol. *24*, 166. https://doi.org/10.1186/s13059-023-02997-8.

41. Cadenas, J., la Cour Poulsen, L., Mamsen, L.S., and Andersen, C.Y. (2023). Future potential of in vitro maturation including fertility preservation. Fertil. Steril. *119*, 550–559. https://doi.org/10.1016/j.fertnstert.2023.01.027.

42. Wigglesworth, K., Lee, K.-B., Emori, C., Sugiura, K., and Eppig, J.J. (2015). Transcriptomic diversification of developing cumulus and mural granulosa cells in mouse ovarian follicles. Biol. Reprod. *92*, 23. https://doi.org/10.1095/biolreprod.114.121756.

43. El-Hayek, S., Demeestere, I., and Clarke, H.J. (2014). Follicle-stimulating hormone regulates expression and activity of epidermal growth factor receptor in the murine ovarian follicle. Proc. Natl. Acad. Sci. USA *111*, 16778–16783. https://doi.org/10.1073/pnas.1414648111.

44. Wang, F., Chang, H.-M., Yi, Y., Li, H., and Leung, P.C.K. (2019). TGF-β1 promotes hyaluronan synthesis by upregulating hyaluronan synthase 2 expression in human granulosa-lutein cells. Cell. Signal. *63*, 109392. https://doi.org/10.1016/j.cellsig.2019.109392.

45. Patton, B.K., Madadi, S., and Pangas, S.A. (2021). Control of ovarian follicle development by TGFβ family signaling. Curr. Opin. Endocr. Metab. Res. *18*, 102–110. https://doi.org/10.1016/j.coemr.2021.03.001.

46. Kim, C.H., Chae, H.D., Cheon, Y.P., Kang, B.M., Chang, Y.S., and Mok, J.E. (1999). The effect of epidermal growth factor on the preimplantation development, implantation and its receptor expression in mouse embryos. J. Obstet. Gynaecol. Res. *25*, 87–93. https://doi.org/10.1111/j.1447-0756.1999.tb01128.x.

47. Thongkittidilok, C., Tharasanit, T., Songsasen, N., Sananmuang, T., Buarpung, S., and Techakumphu, M. (2015). Epidermal growth factor improves developmental competence and embryonic quality of singly cultured domestic cat embryos. J. Reprod. Dev. *61*, 269–276. https://doi.org/10.1262/jrd.2014-167.

48. Kramme, C., Plesa, A.M., Wang, H.H., Wolf, B., Smela, M.P., Guo, X., Kohman, R.E., Chatterjee, P., and Church, G.M. (2021). MegaGate: A toxin-less gateway molecular cloning tool. Star Protoc. *2*, 100907. https://doi.org/10.1016/j.xpro.2021.100907.

49. Danecek, P., Bonfield, J.K., Liddle, J., Marshall, J., Ohan, V., Pollard, M.O., Whitwham, A., Keane, T., McCarthy, S.A., Davies, R.M., et al. (2021). Twelve years of SAMtools and BCFtools. GigaScience *10*, giab008. https://doi.org/10.1093/gigascience/giab008.

50. Zhang, Y., Parmigiani, G., and Evan Johnson, W. (2020). ComBat-seq: batch effect adjustment for RNA-seq count data. NAR Genomics and Bioinformatics *2*, lqaa078. https://doi.org/10.1093/nargab/lqaa078.

51. McInnes, L., Healy, J., and Melville, J. (2018). UMAP: Uniform Manifold Approximation and Projection for Dimension Reduction. J. Open Source Softw. *3*, 861.

52. Traag, V.A., Waltman, L., and van Eck, N.J. (2019). From Louvain to Leiden: guaranteeing well-connected communities. Sci. Rep. *9*, 5233. https://doi.org/10.1038/s41598-019-41695-z.

53. Tang, D., Chen, M., Huang, X., Zhang, G., Zeng, L., Zhang, G., Wu, S., and Wang, Y. (2023). SRplot: A free online platform for data visualization and graphing. PLoS One *18*, e0294236. https://doi.org/10.1371/journal.pone.0294236.

54. Bray, N.L., Pimentel, H., Melsted, P., and Pachter, L. (2016). Near-optimal probabilistic RNA-seq quantifications. Nat. Biotechnol. *34*, 525–527. https://doi.org/10.1038/nbt.3519.

55. Demichev, V., Messner, C.B., Vernardis, S.I., Lilley, K.S., and Ralser, M. (2019). DIA-NN: Neural networks and interference correction enable deep proteome coverage in high throughput. Nat. Methods *17*, 41–44. https://doi.org/10.1038/s41592-019-0638-x.

56. ORFeome Collaboration (2016). The ORFeome Collaboration: a genome-scale human ORF-clone resource. Nat. Methods *13*, 191–192. https://doi.org/10.1038/nmeth.3776.

57. Dobin, A., Davis, C.A., Schlesinger, F., Drenkow, J., Zaleski, C., Jha, S., Batut, P., Chaisson, M., and Gingeras, T.R. (2013). STAR: ultrafast universal RNA-seq aligner. Bioinformatics *29*, 15–21. https://doi.org/10.1093/bioinformatics/bts635.

Please cite this article in press as: Paulsen et al., Development of human induced pluripotent stem cell-derived ovarian support cells as a clinical-grade product for *in vitro* fertilization, Cell Stem Cell (2025), https://doi.org/10.1016/j.stem.2025.12.020

STAR★METHODS

KEY RESOURCES TABLE

REAGENT or RESOURCE	SOURCE	IDENTIFIER
Antibodies		
PE-conjugated mouse monoclonal antibody against CD82	BioLegend	Cat#342104; RRID:AB_1595455
Mouse monoclonal antibody against OCT3/4	Santa Cruz Biotechnology	Cat#sc5279; RRID:AB_628051
Rabbit polyclonal antibody against FOXL2	ABclonal	Cat#A16244; RRID:AB_2769513
Alexa Fluor 555 donkey anti-mouse IgG	Thermo Fisher Scientific	Cat#A32773; RRID:AB_2762848
Alexa Fluor 488 donkey anti-rabbit IgG	Thermo Fisher Scientific	Cat#A32790; RRID:AB_2762833
TRA-1-60 Monoclonal Antibody Alexa Fluor 488	BD Biosciences	Cat#560173; RRID:AB_1645379
Chemicals, peptides, and recombinant proteins		
Pregnant mare serum gonadotropin (PMSG)		N/A
Recombinant follicle-stimulating hormone (rFSH)	Sigma Aldrich	Cat#F4027-2ug
Recombinant follicle-stimulating hormone (rFSH) [Gonal-f]	EMD Serono/Merck	Cat#Gonal-f
Recombinant human chorionic gonadotropin (hCG)	Sigma Aldrich	Cat#CG10
Recombinant human chorionic gonadotropin (hCG) [Ovidrel]	EMD Serono/Merck	Cat#Ovidrel
Androstenedione	Sigma Aldrich	Cat#A-075-1ml
Human serum albumin (HSA)	Life Global	
HSA	CooperSurgical Origio	Cat#ART-3001
Doxycycline	StemCell Technologies	N/A
Doxycycline	Sigma Aldrich	Cat#D5207-5G
Puromycin	Sigma Aldrich	Cat#P9620
Propidium iodide	Sigma Aldrich	Cat#P4864
Triton X-100	Thermo Fisher Scientific	Cat#A16046.AE
Hyaluronidase	Sigma Aldrich	Cat#H3884
Critical commercial assays		
Chromium Single Cell 3′ Library & Gel Bead Kit	10x Genomics	N/A
NEBNext Ultra II Directional RNA Library Prep Kit for Illumina		N/A
NEBNext Multiplex Oligos for Illumina		N/A
NEBNext Poly(A) mRNA Magnetic Isolation Module		N/A
Quick-RNA Microprep Kit	Zymo Research	N/A
LunaScript RT SuperMix Kit	New England Biolabs	N/A
SYBR Green Master Mix	Applied Biosystems	N/A
Quantitative kinetic chromogenic LAL (Limulus Amebocyte Lysate) assay		N/A
PacBio Nanobind PanDNA Kit		N/A
SMRTbell® Prep Kit 3.0		N/A
Doxycycline ELISA	Abcam	Cat#ab285232
Experimental models: Cell lines		
Fibroblast line AG07141	NIA Aging Cell Repository	Cat#AG07141; RRID:CVCL_2C24
RUO-hiPSC line (F66)	Laboratory of G. Church; Pierson Smela et al.[8]	N/A

(*Continued on next page*)

Please cite this article in press as: Paulsen et al., Development of human induced pluripotent stem cell-derived ovarian support cells as a clinical-grade product for *in vitro* fertilization, Cell Stem Cell (2025), https://doi.org/10.1016/j.stem.2025.12.020

CellPress
OPEN ACCESS

Continued

REAGENT or RESOURCE	SOURCE	IDENTIFIER
Female donor hiPSC line (VCT-37-F35)	Reprocell USA; this paper	N/A
Experimental models: Organisms/strains		
Mouse: Hybrid B6/CBA	Janiver Labs	RRID:IMSR_RJ:B6CBAF1
Oligonucleotides		
NR5A1 cDNA	ORFeome Collaboration[48]	EntrezID#2516
RUNX2 cDNA	Pierson Smela et al.[8]	EntrezID#860
GATA4 cDNA	Pierson Smela et al.[8]	EntrezID#2626
Recombinant DNA		
Dox-inducible expression vector	Kramme et al.[22]	Addgene #175503
pCK530_22_NR5A1, NM_004959.9	This paper	N/A
pCK530_33_RUNX2, NM_001024630.4	This paper	N/A
pCK530_3_GATA4, NM_001308093	This paper	N/A
Software and algorithms		
ENSEMBL	Dobin et al.[49]	https://www.ensembl.org/index.html
STAR	Dobin et al.[49]	Version 2.7.10a; https://github.com/alexdobin/STAR
Samtools	Danecek et al.[50]	https://www.htslib.org/
Scapny package	Pedersen et al.[51]	Version 1.9.6; https://scanpy.readthedocs.io/en/stable/
Uniform Manifold Approximation and Projection (UMAP)	McInnes et al.[52]	https://scanpy.readthedocs.io/en/stable/api/generated/scanpy.pl.umap.html
Leiden method	Traag et al.[53]	https://scanpy.readthedocs.io/en/stable/generated/scanpy.tl.leiden.html
Illumina bcl2fastq software	Illumina	Version 2.20; https://support.illumina.com/downloads/bcl2fastq-conversion-software-v2-20.html
Kallisto pseudoalignment discovery	Bray et al.[54]	Version 0.44.0; https://github.com/pachterlab/kallisto
JMP software	SAS Institute Inc.	Version 17; https://www.jmp.com/en/home
SRplot	Tang et al.	https://www.bioinformatics.com.cn/en
DIA-NN	Demichev et al.[55]	Version 1.8; https://github.com/vdemichev/DiaNN/releases
GraphPad Prism software	GraphPad	https://www.graphpad.com/features
Other		
Matrigel	Corning	Cat#354277
Laminin-521	StemCell Technologies	Cat#200-0117
Laminin-511	Reprocell	N/A
NutriStem-XF media	Satorius	Cat#05-100-1A
Y-27632	StemCell Technologies	Cat#72304
CHIR99021	Sigma Aldrich	Cat#SML1046-5MG
iMartix-511	Nippi	Cat#892005
Accutase	StemCell Technologies	Cat#7922
Vitronectin-XF	StemCell Technologies	Cat#7180
CloneR2	StemCell Technologies	Cat#100-0691
CryoStor® CS10	StemCell Technologies	Cat#7930
MediCult IVM Media	CooperSurgical Origio	Cat#82214010D
mTESR1	StemCell Technologies	N/A
TeSR-AOF basal	StemCell Technologies	Cat#100-0402
TeSR-AOF supplemented	StemCell Technologies	Cat#100-0403
HEPES Media [G-MOPS Plus Media]	Vitrolife	Cate#10129
ASP	Vitrolife	Cat#10100

EXPERIMENTAL MODEL AND STUDY PARTICIPANT DETAILS

hiPSC source material

The RUO-hiPSC line was sourced from the laboratory of G. Church; this line is referred to as the F66 line in the reference text.[8] The RUO-hiPSC line was derived from the NIA Aging Cell Repository fibroblast line AG07141 using Epi5 footprint-free episomal reprogramming. A female donor hiPSC line (VCT-37-F35) was sourced from Reprocell USA (9000 Virginia Manor Rd #207, Beltsville, MD 20705) to serve as the starting material for our CG cell line. The parental CG hiPSC starting material was derived from fibroblasts from the skin punch of an eligible United States donor, ID: RPC-VCT-37. Fibroblasts were isolated from a skin punch biopsy and expanded at Reprocell USA (9000 Virginia Manor Rd #207, Beltsville, MD 20705). Donor identity information for 16 loci was obtained by STR analysis performed on donor blood and fibroblasts to confirm sample identity prior to release of the fibroblasts. Fibroblasts were harvested and cryopreserved in cryopreservation containers (ThermoFisher Scientific, catalog number: 377267) in vapor-phased liquid nitrogen (-196°C) to enable testing and further manufacture. The hiPSC line was generated under GMP conditions using a non-integrative, mRNA-based reprogramming technology. The unmodified parental hiPSC line (VCT-37-F35) was characterized by sterility, endotoxin, STR analysis, Karyotype analysis, mycoplasma, viability, phenotype marker, cell purity and morphology, and differentiation testing.

Donor eligibility and cell line manufacturing were performed in line with relevant regulatory standards and guidelines. Regarding specific stages in the manufacturing process, proper controls were implemented for fibroblast derivation according to established guidelines, while reprogramming and cell expansion took place under fully GMP conditions in compliance with regulatory standards and guidelines of the FDA, EMA, and PMDA. Donor eligibility was determined to be in accordance with 21 CFR Part 1271 Subpart C and FDA Guidance for Industry: Eligibility Determination for Donors of Human Cells, Tissues, and Cellular and Tissue Based Products (HCT/Ps), 2021.

hiPSC maintenance and OSC differentiation

hiPSCs were maintained in feeder-free conditions and cell culture plates were pre-coated with either Matrigel (Corning), Laminin-521 (StemCell Technologies), or Laminin-511 (Reprocell). Cells were maintained in either mTESR1 (StemCell Technologies) or TeSR-AOF (StemCell Technologies) without antibiotics at 37 °C in 5% CO2. All hiPSCs were verified for expression of markers associated with pluripotency (TRA-1-60 and TRA-1-81), negative for mycoplasma or other human adventitious agents (performed by IDEXX Bioanalytics), and karyotypically normal (G-band karyotype test, performed by WiCell Research Institute, and Karyostat, performed by ThermoFisher). RUO-hiPSCs and CG-hiPSCs were authenticated by SNP array (CellID, performed by ThermoFisher). All OSC differentiations were initiated from previously characterized hiPSC working banks under passage.[25] Characterization of hiPSC working cell banks includes assessment of marker expression, morphology, vial appearance, container closure integrity, cell count and viability post-thaw, differentiation potential, and testing for endotoxin, mycoplasma, sterility, adventitious agents, and genomic integrity. OSC differentiation was performed as previously described.[8] In short, hiPSCs were exposed to the Rho kinase inhibitor, Y-27632 (StemCell Technologies, 72304), and the WNT activator, CHIR99021 (Sigma Aldrich, SML1046-5MG), to prime the cells into a mesodermal fate. Exposure to doxycycline (Sigma, D5207-5G) throughout the process induced overexpression of the TFs NR5A1, RUNX2, and GATA4. The differentiation process required five days in culture at 37 °C.

Human oocytes for MII maturation assessment

Subjects received three to four days of stimulation using 200 IU of rFSH with a 10,000 IU hCG trigger in preparation for immature oocyte aspiration. Non-contraceptive subjects began stimulation on day 2 of their menstrual cycle, while contraceptive patients began on day 5 following the cessation of pills. Triggers were scheduled when 2 or more follicles reached 6-8 mm in diameter, and average follicle sizes of 6-14 mm were used for extraction 34 to 36 hours after trigger.

Patients were monitored on the day of stimulation start, the day of trigger and the day of oocyte pickup (OPU). During these monitoring periods, transvaginal ultrasound was performed to assess follicle sizes and development. Additionally, serum levels of LH, E2, and P4 were measured to assess the early follicular growth phase (E2 > 100 ng/ml) and to monitor for premature luteinization and spikes in LH (LH $\geq$ 10 IU/ml).

The aspirations of small ovarian follicles to retrieve COCs were performed 34-36 hours after the trigger injection (10,000 IU hCG) using a transvaginal ultrasound with a needle guide on the probe to retrieve oocytes. Aspiration was performed using ASP medium (Vitrolife), a single lumen 19-gauge needle, and 100 mmHg of vacuum pump suction. Follicular aspirates were examined in the laboratory using a dissecting microscope. Aspirates tended to include more blood than typical IVF follicle aspirations, so samples and needles were washed with HEPES media (G-MOPS Plus, Vitrolife) to minimize clotting. Often, the aspirate was additionally filtered using a 70-micron cell strainer (Falcon, Corning) to improve the yield and speed of the oocyte search process. The number of COCs aspirated was equal to roughly 40 to 50% of the subject's AFC.

This study was performed according to the ethical guidelines outlined in the Declaration of Helsinki. Oocyte donor participants were enrolled in the study at several fertility clinics using informed consent for donation of gametes for research purposes, with ethical approval from CNRHA 47/428973.9/22 (Spain), Western IRB No. 20225832 (USA), and Protocol No. GC-MSP-01 (Peru), respectively. These study centers performed the non-clinical research associated with measurement of oocyte maturation endpoints following different IVM regimens, with no subsequent embryo transfer. Information about the ancestry, race, ethnicity, and socioeconomic status of the participants was not collected; therefore, additional data will be needed before comprehensive assessment of the efficacy

Please cite this article in press as: Paulsen et al., Development of human induced pluripotent stem cell-derived ovarian support cells as a clinical-grade product for *in vitro* fertilization, Cell Stem Cell (2025), https://doi.org/10.1016/j.stem.2025.12.020

and safety of *Fertilo* across broader populations. All experiments involving human cells were performed according to ISSCR 2021 guidelines (International Society for Stem Cell Research) and approved by the IRB committees.

Mouse oocytes for the MOMA

Hybrid (B6/CBA) females between 6 and 8 weeks of age, and male mice from the same genetic backgrounds, were purchased from Janvier Labs. Upon arrival, all mice were quarantined and acclimated to the PCB Animal facility (PRAAL) for approximately 1 week prior to use. Mice were housed with a 12-hr light/dark cycle (lights on at 7:00 A.M.) with ad libitum access to food and water. All procedures involving mice, e.g., handling, administration of hormones for superovulation of females were conducted at the PRAAL Animal Facility. Fresh immature mouse oocytes at the germinal vesicle (GV) stage were collected from the ovaries of hybrid (B6/CBA) females between 6 and 8 weeks of age stimulated with 7.5 IU pregnant mare serum gonadotropin (PMSG) 48 hours before retrieval.

All animal care and procedures were conducted according to protocols approved (reference number 10133) by the Institutional Animal Care and Use Committee of Barcelona Science Park de Barcelona (IACUC-PCB), Spain. The PCB Animal Facility is accredited and registered by Generalitat of Catalonia government (B-9900044) as a breeding and user center for laboratory animal research. All protocols carried out in the PCB Animal Facility comply with standard ethical regulations and meet quality and experimental requirements of current applicable National and European legislation (RD 53/2013 Council Directive; 2010/63/UE; Order 214/1997/GC).

Human subjects in the clinical evaluation

A total of 40 female patients were treated under informed consent at two fertility centers in Mexico and Peru. Details about the patient characteristics can be found in Table S6. Information about the ancestry, race, ethnicity, and socioeconomic status of the participants was not collected; therefore, additional data will be needed before comprehensive assessment of the efficacy and safety of *Fertilo* across broader populations. As this clinical study was the first-in-human evaluation of *Fertilo*, only a narrow study population with defined characteristics was included. In Mexico, the product *Fertilo* is approved for commercial use and used in clinical practice. As the patients treated in Mexico were seeking clinical treatment for infertility using a commercially approved product, there was no requirement for ethical approval as the data was requested from the clinical site retrospectively. The study center in Mexico only treated patients as part of the first phase of the study, with no participation in the second randomization phase. For the study center in Peru, which participated in both the first phase and the second phase of the study, which included prospective randomization of patients, Protocol *Fertilo* P1, approved by the ethics committee (CIEI-FMH-USMP, FWA No. 00015320, IRB No. 00003251) was utilized. This evaluation was prospectively registered before recruitment began ISRCTN36032472, with regular IRB updates throughout the two phases as safety and efficacy data became available, to guide treatment in the First in Human evaluation. The protocol, standard operating procedures, and design ensured rigorous oversight and monitoring and compliance with international ethical guidelines.

Inclusion criteria for female patients was as follows: 1. Written informed consent; 2. Premenopausal, age 18-37 years at the time of providing informed consent, who is an appropriate candidate for IVF; 3. Hormone levels within 6 months of consent: follicle stimulating hormone (FSH) level on cycle day 2 or 3 $\geq$ 10 mIU/ml, estradiol (E2) on cycle day 2 or 3 <100 pg/ml, 3. Body Mass Index (BMI) of 21-30 kg/m2; 4. Anti-Müllerian hormone $\geq$ 2 ng/ml and/or Antral Follicle Count $\geq$ 20; 5. No evidence of hormonal disorders as determined by measurements of thyroid stimulating hormone (TSH), prolactin (PRL), sex hormone binding globulin (SHBG) and total testosterone; 6. Normal uterine cavity as assessed by hysteroscopy, hysterosalpingography or sonohysterography within 2 months of screening; 7. Negative and up to date cervical cancer screening (per U.S. Preventive Services Task Force guidelines), all those positive for high-risk human papillomavirus must be negative on subsequent cytology; 8. Presence of both ovaries with no major obstructions (ovarian fibroids, ovarian cysts, high-grade endometriosis); 9. Plan to use one of the resultant embryos within 2 months of egg retrieval; 10. Willing and able to take contraceptives; 11. Male subjects age of 21-45 years; 12. Male subject: provide ejaculated sperm analysis with suitable quality for intracytoplasmic sperm injection (ICSI), these requirements will apply to sperm donors as well; 13. Consent to a study that involves low doses or no doses of gonadotropins followed by retrieval of immature oocytes; 14. Willing to have embryos subjected to PGT-A testing. The exclusion criteria for female patients was as follows: 1. Recurrent pregnancy loss (defined as $\geq$ 2 clinical pregnancies without live birth); 2. Clinical evidence of hormonal etiologies (congenital adrenal hyperplasia, androgen secreting tumors, Cushing's syndrome); 3. Contraindications to being pregnant or to any of the IVF hormonal medications to be used in this study; 4. Presence of uterine anomaly: mullerian defect (septum, didelphic uterus, bicornuate uterus, unicornuate uterus, arcuate uterus); presence of fibroid(s) affecting the endometrium (myoma, leiomyoma); history of thin endometrium (will not become thicker than 6.9 mm with treatment using exogenous gonadotropins and/or exogenous estrogen); asherman syndrome (intrauterine adhesions); 5. Currently taking: lithium, opioids, and/or thyroid medications (other than for treatment of subclinical hypothyroidism) or other known teratogenic medications; 6. Participation in another investigational drug/device trial within previous 30 days of enrollment, or 5 half-lives of the investigational drug, whichever is longer, or planning to participate in an investigational drug/device trial within 30 days of study completion; 7. Greater than 2 previous failed IVF attempts; 8. Known history of oocyte maturation defect or cleavage arrest defect; 9. Tobacco or nicotine use in the past 12 months; 10. History of substance abuse, including alcohol abuse; 11. Abnormal, undiagnosed vaginal bleeding at the time of screening; 12. Abnormal serum iron, HbA1c, prolactin, Hb levels; 13. Any medical or surgical condition that in the Investigator's judgment renders a subject unsuitable for study participation; 14. Inability to comply with study procedures; 15. Condition that requires PGT-M or PGT-SR. Exclusion criteria for male subjects was

as follows: 1. Male: Known or positive test for high DNA fragmentation in sperm; 2. Male: requirement for retrograde ejaculation procedures or surgical sperm retrievals; 3. Sperm Donor: Unsuitable quality for intracytoplasmic sperm injection (ICSI).

Once informed consent was obtained, subjects were screened and evaluated for participation. If required, patients were pretreated for vitamin D deficiency or insulin resistance using calcifediol or metformin respectively before beginning stimulation. Eligible subjects that met all of the inclusion criteria were started on oral contraceptive pills (OCPs) for 10-15 days with a 5-day washout period. For evaluative purposes, the final day of the washout period was considered Day 1 of the menstrual cycle. On Day 2, transvaginal ultrasound (TVU) was performed to assess the antral follicle count (AFC) and follicle diameter for monitoring; in addition, baseline evaluation of serum levels of E2, P4, LH, and FSH were performed via a local laboratory. On Day 2, controlled ovarian stimulation (COS) began via administration of 100 mg clomiphene citrate (Clomid) once daily for 5 days (Day 2-Day 6). Ultrasound was performed on Day 7 to determine the number of 150 IU rFSH (Gonal-F) injections that would be administered. If the leading follicle was 6 mm or less, three once daily injections of rFSH were administered on Days 7, 8, and 9. If follicles were 7 mm to 9 mm on Day 7, 150 IU (Gonal-F) was administered once daily on Day 7 and 8, for a total of two injections. If the leading follicle was greater than 9 mm on Day 7, a single injection of 150 IU (Gonal-F) was administered on Day 7.

The ideal leading follicle diameter range was 10-12 mm. On Day 8, 9 or 10, a recombinant hCG (Ovidrel) trigger of 250 μg was administered and the oocyte retrieval (OR) was scheduled for 34-36 hours later. In the event of rapid follicular growth, if a follicle was 13 mm or greater at the Day 2 or Day 7 ultrasound, the cycle was cancelled and repeated in a subsequent menstrual cycle.

In the observational safety phase, all twenty subjects were assigned to OSC-IVM (*Fertilo*) treatment. For the control comparator phase, patients were randomized at a 1:1 ratio to OSC-IVM (*Fertilo*) or Traditional IVM (Media Only IVM) on the day of hCG trigger. Oocyte retrieval was performed according to standard clinical practice using a 17-gauge single lumen needle with 70 mm Hg suction pressure. Rapid needle movement (curettage) was performed to improve oocyte extraction from the follicular wall. All oocyte retrievals were performed under anesthesia. Oocytes were collected into warmed collection media containing heparin in order to minimize clotting. Further, tubing length was minimized and the needle was flushed every 4-5 punctures to minimize clotting and temperature fluctuations during retrieval. No follicular flushing was performed in any retrieval cycle.

METHOD DETAILS

Plasmid manufacturing

Plasmids utilized for engineering the CG-hiPSC line to direct differentiation into OSCs were manufactured as previously described.[8] Briefly, transcription factor cDNAs (*NR5A1*, *RUNX2*, and *GATA4*) were obtained as Gateway entry clones from the ORFeome[56] or cloned as custom gene blocks. These sequences were cloned into a barcoded Dox-inducible expression vector (Addgene #175503) using MegaGate cloning.[48] The final *NR5A1*, *RUNX2*, and *GATA4* plasmids (pCK530_22_NR5A1, NM_004959.9; pCK530_33_RUNX2, NM_001024630.4; and pCK530_3_GATA4, NM_001308093) were subjected to whole plasmid sequencing via Plasmidsaurus using Oxford Nanopore Technology with custom analysis and annotation. All plasmids were screened for purity and stored at -20°C, while glycerol stocks of transformed bacteria were stored at -80°C.

Cell engineering

The CG-hiPSC line was engineered to harbor doxycycline-inducible transcription factors to enable directed differentiation into OSCs. The parental GMP hiPSC clone VCT-37-F35 was thawed at 37°C and resuspended in NutriStem-XF media (Satorius, 05-100-1A) supplemented with Y-27632 (STEMCELL Tech, 72304). Cells were centrifuged and the supernatant was removed. Then, pelleted cells were again resuspended in NutriStem-XF media (Satorius, 05-100-1A) supplemented with Y-27632 (STEMCELL Tech, 72304) and cell count and viability were assessed. Cells were then seeded onto flasks pre-coated with iMatrix-511 (Nippi, 892005) and incubated for 6 days at 37ºC. To adapt hiPSCs to the media and substrate, cells were cultured for 3 passages, during which cell quality was monitored based on morphology and confluency; for each round of expansion, Accutase (STEMCELL Tech, 7922) was used to facilitate cell detachment from flasks, and cell count and viability were assessed. Parental hiPSCs (VCT-37-F35) at passage 11 (day 16) were assessed for confluency, detached using Accutase (STEMCELL Tech, 7922), centrifuged, resuspended in TeSR-AOF supplemented with Y-27672 (STEMCELL Tech, 100-0403), and cell count and viability were assessed. Resuspended cells were centrifuged and resuspended in electroporation buffer (P3 solution, P3 Lonza Nucleofection Kit, V4XP-3024) with equimolar quantities of the 3 plasmids encoding the transgenes *NR5A1*, *RUNX2*, and *GATA4* (pCK530_22_NR5A1, pCK530_33_RUNX2, and pCK530_3_GATA4) in addition to the PiggyBac transposase plasmid (pAMP470 pBASE-Super PiggyBac Transposase). Delivery of the plasmids into the cells was performed using the Lonza 4D-Nucleofector Unit set to the CM-113 program. Transfected cells were plated (100,000 cells/cm^2) into a well of a 24-well plate pre-coated with Vitronectin-XF (STEMCELL Tech, 7180) and cultured with TeSR-AOF supplemented with Y-23672 (STEMCELL Tech, 100-0403). For the next four days (days 17-20), daily media changes with TeSR-AOF (STEMCELL Tech, 100-0402) supplemented with Puromycin (Sigma-Millipore, P9620-10ML) were performed for selection; cell quality was monitored by morphological and confluency checks. The following four days (days 20-24), resistant cells were maintained with TeSR-AOF with no supplementation (STEMCELL Tech, 100-0402). On day 24, expanded resistant cells were detached from the flasks using Accutase (STEMCELL Tech, 7922), centrifuged, and resuspended into TeSR-AOF supplemented with Y-23672 (STEMCELL Tech, 100-0403). The cells from one well of the 24-well plate (1.9 cm^2) were further expanded into two wells of a 6-well plate (19.2 cm^2). From days 25-27, daily media changes with TeSR-AOF (STEMCELL Tech, 100-0402) supplemented with Puromycin (Sigma-Millipore, P9620-10ML) were conducted, and cell quality was monitored by morphological and confluency checks.

Please cite this article in press as: Paulsen et al., Development of human induced pluripotent stem cell-derived ovarian support cells as a clinical-grade product for *in vitro* fertilization, Cell Stem Cell (2025), https://doi.org/10.1016/j.stem.2025.12.020

On day 28, clonal selection was performed by limiting dilution of cells on TeSR-AOF (STEMCELL Tech, 100-0402) supplemented with CloneR™2 (STEMCELL Tech, 100-0691). Single cells were plated onto Vitronectin-XF (STEMCELL Tech, 7180). During clonal expansion (days 29-34), individual wells were carefully monitored to assess colony morphology, growth/confluency, and confirm the presence of a single colony per well. TeSR-AOF (STEMCELL Tech, 100-0402) media changes were performed daily until ready for colony selection. Between days 35-46, once a clone had reached significant levels of expansion (< 10 days after seeding), the individual well was treated with Accutase (STEMCELL Tech, 7922) to promote cell detachment. Cells were centrifuged, resuspended in TeSR-AOF supplemented with Y-23672 (STEMCELL Tech, 100-0403), and seeded onto one well of a 24-well plate pre-coated with Vitronectin-XF (STEMCELL Tech, 7180). When a given clone was ready to be passed, the same procedure was repeated and expanded cells were plated onto a 6-well plate pre-coated with Vitronectin-XF (STEMCELL Tech, 7180). During this expansion, all clones were screened for integration of the three transcription factors (*NR5A1*, *RUNX2*, and *GATA4*). In addition, TF insertion sites were verified by Whole Genome Sequencing (Azenta). The analysis showed no evidence of mutations in 20 common proto-oncogenes. Expanded cells were treated with Accutase (STEMCELL Tech, 7922), centrifuged, and the supernatant was removed. Cells from each clone were resuspended in CryoStor® CS10 (STEMCELL Tech, 7930), gently mixed, and filled into cryovials. The finished vials were cryopreserved in a Mr. FrostyTM freezing container at -80°C freezer for a maximum of 24 hours. The cryopreserved cells were stored in cryopreservation containers (Azenta Life Sciences, catalog number: 67-0755-11) and transferred to vapor-phase liquid nitrogen (-196°C) with temperature monitoring for long-term storage.

Cell screening and clone selection

To identify the optimal hiPSC clone for downstream development, after seed hiPSC clones were assessed by genotyping PCR to verify the presence of the three TFs, nine clones harboring all the TFs were identified and each clone was subjected to a more in-depth screening process. To identify the lead candidate, each of the nine clones was individually differentiated and subjected to a series of assays to ensure identity (pluripotency markers, and genotyping), conformance (cell count and viability), and potency (OSC production and function). The leading candidate clone (2-D10) selected to be used as the starting material for the CG cell line was named CG-hiPSC.

Cell count and viability

Cell counting and viability assessment were performed to establish the number of live cells utilized for initial testing. Cell count and viability assessment were performed using an Eve Automated Cell Counter (NanoEnTeck) and a NucleoCounter NC-202 (ChemoMetec), respectively.

Single cell RNA sequencing (scRNA-seq)

scRNA-seq was performed to establish comparability between resultant OSCs that were generated under various differentiation conditions, as well as evaluate the consistency of different batches generated using the same condition. OSCs were cryopreserved in CryoStor CS10 (StemCell Technologies) prior to being processed for single-cell RNA sequencing by Genewiz (Azenta). Cells were loaded onto a Chromium Single Cell Chip (10x Genomics) and processed through the Chromium Controller to generate single-cell gel beads in emulsion. scRNA-seq libraries were generated using the Chromium Single Cell 3′ Library & Gel Bead Kit (10x Genomics). Target cell recovery was estimated to be 3,000 cells per sample. Files were generated following a split-set analysis workflow. First bcl2fastq was used to generate the fastq files. Next, a reference genome was generated using split-pipe and the Homo sapiens GRCh38 file, also using STAR[57] and Samtools.[49] Then, split-pipe was run to process and align the files against the reference genome. The resulting files were generated in an mtx matrix format. Finally, the files were combined, and an Anndata object was made in h5ad file format. For the analysis, cells with less than 200 genes were filtered out, as well as genes found in less than 3 cells. Cell counts were normalized to 10,000 Unique molecular identifiers (UMIs) per sample and log (ln) plus 1 transformed. Principal component analysis was performed using the Scanpy package (v1.9.6) based on 30 PCA components, and using PCA results, nearest neighbor analysis was performed using n_neighbors = 20. Batch correction was performed using Scanpy's ComBat method.[50] The number of components used for batch correction was 30 and the data was then transformed using the Uniform Manifold Approximation and Projection (UMAP) method.[51] Clusters were formed using the Leiden method[52] with a resolution of 0.25 for the complete dataset (containing all lots described in the manuscript), and projected into the subsetted objects. At first, 15 Leiden clusters were identified. Thereafter, clusters were combined based on biological similarities, which resulted in nine final clusters: Early GC I, Early GC II, Early GC III, GC I, GC II, GC III, Atresia/luteolysis, Mitochondrial gene enriched (Atresia/luteolysis), and Ribosomal gene enriched (Atresia/luteolysis). The marker genes per cluster, as well as certain granulosa cell markers (*GJA1, MDK, BBX, HES4, PBX3, YBX3, BMPR2, CD46, COL4A1, COL4A2, LAMC1, ITGAV*, and *ITGB1*), were analyzed to identify cluster cell types. Dot plots and feature plots were generated to assess the expression levels of certain genes per cluster or per sample. Based on downstream analysis, clusters 0 and 5 were subsetted from the original object and they were re-clustered using the Leiden method at a higher resolution of 0.3. Subclusters were combined based on biological similarities. Once all the subgroups were identified, the subclusters resulting from cluster 0 and cluster 5 were merged with the original object. Gene signatures based on genes in the folliculogenesis stage[21] were also analyzed and used in predicting cluster identification. Signature scores for the RUO-OSC-M subset were generated for two groups: Antral and Pre-Ovulatory genes. Based on the final object, 4 more subsets were generated: (1) a RUO-OSC-M object consisting of the following lots: lot 6, lot 7, lot 8, lot 29, lot 48, and lot 56; (2) a RUO-OSC-L object consisting of lot 77 and lot 86; and (3) a CG-OSC-L object consisting of lot 88 and lot 90. UMAPs of all the subsets were generated with the cluster names from the original object.

Please cite this article in press as: Paulsen et al., Development of human induced pluripotent stem cell-derived ovarian support cells as a clinical-grade product for *in vitro* fertilization, Cell Stem Cell (2025), https://doi.org/10.1016/j.stem.2025.12.020

Bulk RNA-sequencing

Bulk RNA-sequencing was performed to detect the expression of well-known granulosa cell markers among resultant OSCs as a measure of successful differentiation. hiPSCs were differentiated into *Fertilo* OSCs following a 5 day differentiation protocol with exposure to doxycycline (Sigma, D5207-5G). Libraries for RNA sequencing were generated using the NEBNext Ultra II Directional RNA Library Prep Kit for Illumina (NEB #7765L) in conjunction with NEBNext Multiplex Oligos for Illumina (Unique Dual Index UMI Adaptors RNA Set1, NEB #7416S) and NEBNext Poly(A) mRNA Magnetic Isolation Module (NEB #E7490L), according to the manufacturer's instructions. The library pool was sequenced at Azenta using Illumina 2x150 bp, ~350 M PE reads (~105 GB), lightening package. Illumina sequencing files (bcl-files) were converted into fastq read files using Illumina bcl2fastq (v2.20) software deployed through BaseSpace using standard parameters. RNA-seq data gene transcript counts were aligned to *Homo sapiens* GRCH38 (v2.7.4a) genome using STAR (v2.7.10a)[57] to generate gene count files and annotated using ENSEMBL.[57] Gene counts were combined into sample gene matrix files (h5). Computational analysis was performed using the Scanpy (v1.9.6) package. Two h5ad files were joined based on similar features and genes. The two merged files were created into one Anndata object which was normalized to 10,000 UMI per sample and log (ln) plus 1 transformed. Principal component analysis was performed using 30 PCA components. Projection into two dimensions was performed using the UMAP method.[51] This analysis was performed to evaluate the CG-hiPSC sub-clones: 2-A7, 2-C9, 2-D10, 2-G1, 2-G11, 2-H10, 3-C7, 3-D3, and 3-E3.

Barcode-Seq of residual OSC presence

Barcode-seq was performed to ensure the absence of any residual OSC material in oocytes following IVM with *Fertilo*. hiPSCs were differentiated into *Fertilo* OSCs following a 5 day differentiation protocol with exposure to doxycycline (Sigma, D5207-5G). Following IVM, low input bulk RNA sequencing of individual mature oocytes was performed using the NEB Low Input RNA-seq library preparation kit and sequenced on an Illumina MiSeq by Genewiz (Azenta). Two reference positive control samples of RUO-OSCs were directly sequenced to serve as controls, using the same library preparation and sequencing kit. Additionally, two negative control samples of patient derived cumulus cells were used as a somatic cell negative control and likewise prepared using the same library preparation and sequencing kit. All samples were assessed for RNA integrity scores (RIN) of greater than 8 and sequenced to the same depth.

In order to determine the residual presence of OSCs using RNA-sequencing, a set of sequences unique to OSCs was utilized as a target for assessment. This unique sequence consists of a 20 base pair barcode that is expressed uniquely on the 3' untranslated region (UTR) or the exogenous transcription factors (TF) used to manufacture *Fertilo* OSCs.

Barcode identification was performed on Fastq files using the following method. Briefly, a Kallisto reference genome library was built using Kallisto index, depending on target sequences, using kmers = 15 to kmers =31. An index on specific barcode sequences and flanking regions downstream of inserted TF sequences was included. Additionally, an index reference genes (KRT19 and EpCAM) known to be active in OSC lines and oocyte cells was included. Kallisto sudo alignment of transcriptomic read files (FASTQ) to kallisto genomic index was performed. Read counts were then collected and compared of barcode sequences found downstream of inserted synthetic transcription factor (TF) genes.

To ensure the oocytes were sequenced with enough depth and were not negative due to low read depth, two highly expressed housekeeping genes were likewise analyzed, KRT19 and EpCAM, to filter samples with unsuitably low read depth. These housekeeping genes were chosen for their conserved expression in both oocytes and reference somatic cell and *Fertilo* OSC controls. Relative quantification of the barcodes and gene sequences of interest were performed using kallisto pseudoalignment discovery (v 0.44.0)[54] and expressed as a transcript per million (TPM) measure.

To select barcodes that are sensitive and specific to detection of *Fertilo* OSCs, three 20 bp barcodes, with 2 kmer lengths, as well as the endogenous gene were evaluated for sensitivity and specificity. Sensitivity was assessed as being detectable in the reference RUO OSC positive control sample. Specificity was assessed as being detectable in the reference RUO OSC positive control sample and undetectable in the cumulus cell somatic negative control.

For analysis of residual *Fertilo* OSCs in embryo samples, the preimplantation genetic testing for aneuploidy (PGT-A) of trophectoderm biopsies was utilized. The platform utilized for PGT-A utilized microarray analysis (Juno Genetics) on 4 to 8 cell biopsy samples. The analysis utilized single nucleotide polymorphisms (SNPs) and haploblock mapping to determine whether the biopsy sample is euploid, aneuploid, segmental aneuploid, or mosaic. Furthermore, for each embryo, a sample of maternal blood and paternal sperm were utilized to compare the SNPs of the embryo to the SNPs of the maternal and paternal donors. Furthermore, a sample of RUO OSCs was provided to determine the SNP profile of residual RUO OSCs. Therefore, through analysis of the embryo's SNPs presence of maternal, paternal, and residual *Fertilo* OSC DNA could be accurately identified in parallel to aneuploid status. For all biopsies, day 3 laser-assisted zona drilling was performed, and biopsies were performed on embryos that reached transferable quality grade on day 5 through 7 of development, as determined by the Gardner Score of 3BB or greater.

Design of Experiments (DOE)

A DOE was performed to identify the optimal differentiation conditions for manufacturing. DOE was conducted using JMP software (JMP 17, SAS Institute Inc., Cary, NC, USA) to optimize experimental parameters, including media supplementation, substrates, and doxycycline treatment designs. Factors were selected from established modulators for OSC specification and factor ranges were determined through literature review (Table S3). Responses were FOXL2 expression and viability. Viability was used to screen and remove experimental groups below 50% cell survival prior to the final statistical analysis. A custom design was employed

Please cite this article in press as: Paulsen et al., Development of human induced pluripotent stem cell-derived ovarian support cells as a clinical-grade product for *in vitro* fertilization, Cell Stem Cell (2025), https://doi.org/10.1016/j.stem.2025.12.020

and optimized for D-optimality to investigate main effects and interactions. JMP software facilitated generation of the experimental design matrix, as well as statistical analysis through response surface methodology (RSM), ANOVA, and optimization of conditions to maximize response desirability for FOXL2 expression.

A DOE was performed to identify optimal differentiation conditions for OSC manufacturing. DOE was conducted using JMP Pro (JMP 17, SAS Institute Inc., Cary, NC, USA) to systematically evaluate the effects of media supplementation, substrate conditions, and doxycycline treatment parameters on OSC specification. Experimental factors were selected from established modulators of granulosa-cell differentiation and factor ranges were defined through literature review (Table S3). The primary responses were FOXL2 expression and cell viability, quantified by flow cytometry. Experimental groups exhibiting less than 50% viability were excluded prior to statistical modeling.

A custom experimental design was generated in JMP to characterize the contributions of a broad panel of differentiation variables. The design incorporated 18 total factors, including four categorical variables (basal media type, percentage of KnockOut Serum Replacement (KSR), presence or absence of nonessential amino acids (NEAA), and substrate type) and fourteen continuous supplements (sodium pyruvate, 2-mercaptoethanol, doxycycline concentration, doxycycline exposure time, CHIR99021, BMP4, LDN, FGF9, PD0325901, and SAG, each varied across the ranges specified in the experimental matrix). Continuous factors were modeled as numeric variables, and center points were included to allow assessment of curvature. A single interaction term between doxycycline concentration and exposure time was incorporated based on expected mechanistic dependence between these parameters.

A custom A-optimality criterion was used to maximize the precision of estimated main effects while maintaining design efficiency. The final design consisted of 32 experimental conditions. All conditions were plated and processed using standardized workflows, and all flow-cytometry measurements were performed on the same instrument. Technical replicates present within the design were included in model fitting but were not treated as separate block or batch terms.

Model fitting was performed using the standard least-squares platform in JMP, including all main effects and the prespecified doxycycline concentration × doxycycline time interaction. Model construction, variance estimation, and statistical testing were conducted within JMP's analytic framework, which included generation of the experimental design matrix, ANOVA-based evaluation of fitted models, and response surface methodology to support the optimization of differentiation conditions.

Proteomics

Proteomics analysis was performed to compare the differently regulated proteins in RUO-OSCs and CG-OSCs at 24 hours versus OSCs at 0 hours, as well as the differently regulated proteins in RUO-OSCs and CG-OSCs versus hiPSCs. In addition, proteomic analysis of conditioned media was utilized for secretome analysis of RUO-OSCs versus CG-OSCs. Liquid chromatography followed by tandem mass spectrometry (LC-MS/MS) analysis was conducted on a series of samples, including RUO-hiPSC (n=1), CG-hiPSC (n=1), RUO-OSC-M lot 56 at time 0h (n=1) and after 24h (n=1) of culture with supplemented IVM media, and CG-OSC-L lot 88 at time 0h (n=1) and after 24h (n=1) of culture with supplemented IVM media. Each condition involved the analysis of 2 million cells. Supplemented IVM media consisted of MediCult IVM media (CooperSurgical Origio) supplemented with 75 mIU/mL of recombinant FSH (Sigma), 100 mIU/mL recombinant hCG (Sigma), 500 ng/mL of androstenedione (Sigma), 1 ug/mL of doxycycline (Sigma) and 10 mg/mL of human serum albumin (HSA; CooperSurgical Origio). Conditioned media derived from RUO-OSC-M lot 56 (n=1) and CG-OSC-L lot 88 (n=1) were also analyzed. To generate conditioned media, 2 million OSCs were cultured in 2 mL of supplemented IVM media for 24 hours, maintaining the ratio of the intended clinical cell dose of 1,000 OSC cells per 1 μL of media. The 24-hour culture was performed with CO_2 set for a pH of 7.2-7.4.

Following culture, OSCs and conditioned media were separated and processed independently. Supplemented IVM media without OSCs was used as a media control. The conditioned media were subjected to consecutive centrifugations (300 x g, 1,200 x g, and 3,000 x g) to remove cellular remnants, and then passed through albumin depletion columns (AVK-50, AlbuVoid Albumin Depletion Columns Biotech Support Group) to eliminate HSA-derived albumin. Proteins from cells and conditioned media were precipitated using acetone, re-suspended in 0.1% RapiGest and 25 mM ammonium bicarbonate, reduced with DTT, and alkylated with iodoacetamide, before undergoing in-solution trypsin digestion overnight at 37°C. The resulting peptides were desalted using C18 stage-tip columns prior to analysis using a Thermo Fisher Scientific EASY-nLC 1200 coupled online to a Fusion Lumos mass spectrometer (Thermo Fisher Scientific).

For LCMS/MS analysis, buffer A (0.1% FA in water) and buffer B (0.1% FA in 80 % ACN) were used as mobile phases for gradient separation. For peptide separation, a packed in-house 75 μm x 15 cm chromatography column (ReproSil-Pur C18-AQ, 3 μm, Dr. Maisch GmbH, German) was used. Peptides were separated with a gradient of 5–40% buffer B over 30 min, and 40%-100% B over 10 min at a flow rate of 400 nL/min. Fusion Lumos mass spectrometer operated in a data independent acquisition (DIA) mode, collecting MS1 scans in the Orbitrap mass analyzer from 350-1400 m/z at 120K resolutions. The instrument was set to select precursors in 45 x 14 m/z wide windows with 1 m/z overlap from 350-975 m/z for HCD fragmentation. MS/MS scans were collected in the orbitrap at 15K resolution. Data analysis involved searching against human Uniprot database (8/7/2021) using DIA-NN v1.8[55] with filtering for 1% false discovery rate (FDR) for both protein and peptide identifications. Protein intensities were normalized and log transformed for relative quantitation, and multiple hypothesis correction of p-values was performed using the Benjamini-Hochberg method. Proteomic analyses were conducted at the Proteomics and Metabolomics Core Facility at Weill Cornell Medicine (New York, USA). GO Chord graphs generated with the free online platform, SRplot.[53]

Please cite this article in press as: Paulsen et al., Development of human induced pluripotent stem cell-derived ovarian support cells as a clinical-grade product for *in vitro* fertilization, Cell Stem Cell (2025), https://doi.org/10.1016/j.stem.2025.12.020

Flow cytometry

Flow cytometry analysis was performed to assess the presence of hiPSCs and granulosa-like cells in different batches of OSCs. Flow cytometry analyses were conducted on live and fixed RUO-OSC and CG-OSC samples. For the analysis of live cells, cells were incubated with a PE-conjugated mouse monoclonal antibody against CD82 (1:50 dilution; 342104, BioLegend) in FACS wash (dPBS with 5% fetal bovine serum (FBS)). After incubation, cells were washed with FACS wash, stained with propidium iodide (1:20 dilution; P4864, Millipore Sigma) for live/dead staining, and subsequently analyzed using a CytoFlex Flow Cytometer. For the analysis of fixed cells, cells were fixed with 4% PFA for 15 minutes at RT and then washed with dPBS. After, cells were permeabilized using FACS wash solution containing 0.1% Triton X-100 (A16046.AE, Thermo Fisher Scientific). The primary antibodies were mouse monoclonal antibody against OCT3/4 (1:50 dilution; sc5279, Santa Cruz Biotechnology) and rabbit polyclonal antibody against FOXL2 (1:100 dilution; A16244, ABclonal). The secondary antibodies were Alexa Fluor 555 donkey anti-mouse IgG (A32773, Thermo Fisher Scientific), and Alexa Fluor 488 donkey anti-rabbit IgG (A32790, Thermo Fisher Scientific). Following incubations, cells were washed with FACS wash containing Triton X-100 and then analyzed using a CytoFlex Flow Cytometer. Unstained cells (negative controls) were used to determine the gating strategy.

For analytical testing, hiPSCs were stained with Alexa Fluor 488-conjugated TRA-1-60 antibody (1:100 dilution; TRA-1-60 Monoclonal Antibody Alexa Fluor 488, BD Biosciences, Cat.#: 560173) for 1 hour on ice. Subsequently, cells were stained with propidium iodide (1:20 dilution; Sigma, Cat.#: P4864) right before analysis to distinguish live/dead cells. A total of $\geq$ 30,000 TRA-1-60+ live cells were acquired on a CytoFLEX S Flow Cytometer and the data was analyzed using FlowJo 10.10.0. The gating strategy was defined using an unstained hiPSC sample.

RT-qPCR and genotyping PCR

Genotyping PCR was performed to assess the presence of the engineered transcription factors in hiPSC clones. For genotyping PCR, DNA extraction from various hiPSC clones was carried out using the QuickExtract DNA Extract Solution (Epicentre), following the manufacturer's instructions. PCR amplification was performed using Q5 High-Fidelity 2X Master Mix (New England Biolabs) for 35 cycles with a 20-second extension time. Subsequently, PCR was performed to validate the integration of the 3 TFs *NR5A1*, *GATA4*, and *RUNX2*. The PCR protocol involved an initial denaturation step at 98°C for 30 seconds, followed by 35 cycles of denaturation at 98°C for 10 seconds, annealing at 66-70°C (*NR5A1*, 67°C; *RUNX2*, 66°C; *GATA4*, 70°C) for 10 seconds, and extension at 72°C for 20 seconds, with a final extension step of 2 minutes. The reaction was then held at 4°C. Gel electrophoresis (2% agarose) was performed to confirm the presence of TFs.

RT-qPCR was performed to assess the presence of residual pluripotent cells in OSCs post-differentiation based on gene expression of *OCT4* and *NANOG*, following protocol recommendations from the New York Stem Cell Foundation (NYSCF). RNA extraction was performed using the Quick-RNA Microprep Kit (Zymo Research) following the manufacturer's instructions. cDNA synthesis was carried out with the LunaScript RT SuperMix Kit (New England Biolabs). Quantification of RNA and cDNA was performed using Nanodrop. PowerUp SYBR Green Master Mix (Applied Biosystems) was used for RT-qPCR. For RT-qPCR, the thermocycler program consisted of a primer annealing stage at 25°C for 2 minutes, followed by cDNA synthesis at 55°C for 10 minutes, concluded with heat inactivation at 95°C for 1 minute. The RT-qPCR protocol involved an initial denaturation step at 95°C for 2 minutes, followed by 40 cycles of denaturation at 95°C for 3 seconds, annealing at 60°C for 30 seconds, and an analysis step.

Functional assessment (oocyte maturation)

The function assessment was performed to determine the oocyte maturation-stimulating potential of various OSC batches. Briefly, human immature oocytes surrounded by cumulus cells, known as cumulus-oocyte complexes (COCs), were retrieved from subjects that underwent minimal stimulation protocols. Subsequently, these immature COCs were co-cultured with different batches of OSCs for 24-30 hours to facilitate IVM. After IVM, oocytes were evaluated for their maturation state and categorized into immature stages (GV oocyte or MI oocyte) or mature stage (MII oocytes). MII oocyte maturation rate (%) was calculated by dividing the total number of mature MII oocytes by the initial number of immature oocytes; MII oocyte maturation rate was used as the potency readout. For a comprehensive description of the methods follow, refer to our recent publication.[17] The number of oocyte donor participants and the total number of oocytes used per OSC batch assessed are detailed in Table S7.

Control conditions for hiPSC manufacturing

The control conditions for hiPSC manufacturing were established to enable the generation of the clinically suitable product. The controlled conditions used for manufacturing were established based on the current Good Manufacturing Practice (cGMP) conditions outlined in 21 CFR Parts 210 and 211 with a focus on use of suitable materials, implementation of contamination and cross contamination controls, and adherence to standard operating procedures. Briefly, a quality control unit was established at Gameto and all personnel and consultants met qualifications for assigned functions; all buildings and facilities were deemed suitable for manufacturing; equipment was determined to be appropriate for use with detailed maintenance and cleaning procedures; raw materials were received, stored, handled, and tested appropriately; standard operating procedures for production and processing were written and executed, and deviations were reported; packaging, labeling, holding, and distribution procedures were put in place; and protocols for salvaged drug products were developed. In addition, suitable laboratory controls, as well as procedures for maintaining records and generating reports, were established.

Please cite this article in press as: Paulsen et al., Development of human induced pluripotent stem cell-derived ovarian support cells as a clinical-grade product for *in vitro* fertilization, Cell Stem Cell (2025), https://doi.org/10.1016/j.stem.2025.12.020

Safety testing

Safety testing of the clinical product was performed to ensure that *Fertilo* met all regulatory standards to allow for clinical application.

Mycoplasma testing was performed on OSCs in duplicate. Mycoplasma testing included detection of the presence of *Mycoplasma pulmonis* and *Mycoplasma sp*. DNA was extracted and real-time quantitative polymerase chain reaction (RT-qPCR) was used for the direct detection of nucleic acid sequences for the mycoplasma targets. In addition, mycoplasma testing was also performed on cell culture supernatant collected during harvesting day. Cell culture supernatant was inoculated into a single flask containing sterile complete mycoplasma broth. The flask was incubated under microaerophilic conditions at 36°C ± 1°C under 5-10% CO_2 in nitrogen for 7 days. Broth culture was collected, RNA was isolated, and RT-qPCR was then performed to amplify and detect nucleic acid sequences from organisms within the class Mollicutes, including mycoplasma species and related *Acholeplasma laidlawii*.

Endotoxin testing was performed on thawed hiPSC or OSC samples using a quantitative kinetic chromogenic LAL (Limulus Amebocyte Lysate) assay in accordance with the USP <85> compendial method.

Sterility testing was performed in accordance with the USP <71> compendial method to detect bacteria and fungi. Samples are aseptically directly inoculated onto vessels containing Fluid Thioglycollate Medium (FTM) and Soybean Casein Digest Medium (SCDM)/Tryptic Soy Broth (TSB). Two vessels containing uninoculated FTM and two vessels containing uninoculated SCDM/TSB serve as negative controls. FTM vessels are placed at 31°C – 35°C for 14 days, whereas SCDM/TSB vessels are placed at 21°C – 25°C for 14 days. All vessels are observed for evidence of growth on days 3, 4 or 5, day 7 or 8, and day 14. The test is considered valid if no growth is observed in the negative controls.

Adventitious agents (human test panel) testing was performed on hiPSCs and OSCs. Adventitious agents (human test panel) testing included detection of the presence of the most common human adventitious agents: Hepatitis A, Hepatitis B, Hepatitis C, HTLV Type I & II and STLV Type 1, Human Immunodeficiency Virus Type 1, Human Immunodeficiency Virus Type 2, Epstein Barr Virus, Human Cytomegalovirus, Human Herpesvirus Type 6, Human Herpesvirus Type 7, Human Herpesvirus Type 8, Parvovirus B19, JC Virus, and BK Virus. DNA is extracted, and real-time quantitative polymerase chain reaction (qPCR) is used for the direct detection of nucleic acid sequences for Hepatitis B, Epstein Barr Virus, Human Cytomegalovirus, Human Herpesvirus Type 6, Human Herpesvirus Type 7, Human Herpesvirus Type 8, Parvovirus B19, JC Virus, and BK Virus. RNA is extracted, and real-time reverse transcription quantitative polymerase chain reaction (RTqPCR) is used for the direct detection of nucleic acid sequences for Hepatitis A, Hepatitis C, HTLV Type I & II and STLV Type 1, Human Immunodeficiency Virus Type 1, and Human Immunodeficiency Virus Type 2.

Genomic integrity of hiPSCs and OSCs is assessed through whole genome sequencing (WGS). Sample processing is performed using the PacBio Nanobind PanDNA Kit, followed by library preparation with the SMRTbell® Prep Kit 3.0. Sequencing is then conducted on the PacBio Revio, a long-read sequencing system that utilizes single-molecule real-time (SMRT) sequencing technology by Genewiz (Azenta). To evaluate genome-wide DNA alterations that may have arisen during the manufacturing of hiPSC banks and *Fertilo* OSC lots, variant calling analysis is performed. The effects of detected variants on transcripts are annotated and predicted using Ensembl. Comparisons are made between the test sample DNA and the GRCh38 reference genome, with intersection tests conducted for single nucleotide polymorphisms (SNPs), insertions/deletions (INDELs), and structural variants (SVs).

The presence of residual hiPSCs in the test article (*Fertilo*) is assessed by RT-qPCR targeting the pluripotent stem cell markers *OCT4* and *NANOG*. GAPDH serves as a housekeeping gene for normalization. The acceptance criteria for residual hiPSC testing is "*OCT4* $\leq$ 0.1% and *NANOG* $\leq$ 0.1%".

Residual doxycycline was performed on OSC samples. Exposure to doxycycline throughout the hiPSC differentiation process induces overexpression of the transcription factors, NR5A1, RUNX2, and GATA4, directing differentiation of hiPSCs towards OSCs. To confirm that doxycycline is not carried over into the final product, an ELISA against doxycycline (Abcam, Cat. #ab285232) was performed on conditioned media.

Embryotoxicity is tested using a mouse embryo assay (MEA) to confirm that *Fertilo* does not cause harm to embryos or gametes, following the FDA guidance recommendations on conducting "Mouse Embryo Assay for Assisted Reproduction Technology Devices". At the completion of embryo culture, blastocysts formation rate (BFR) is assessed, and the acceptance criteria is $\geq$ 80% embryos successfully developed into blastocysts.

Murine oocyte maturation assay (MOMA)

The MOMA was performed as a measure of the potency of different lots of OSCs. Hybrid (B6/CBA) females, and male mice from the same genetic backgrounds, were purchased from Janvier Labs. Upon arrival, all mice were quarantined and acclimated to the PCB Animal facility (PRAAL) for approximately 1 week prior to use. Mice were housed with a 12-hr light/dark cycle (lights on at 7:00 A.M.) with ad libitum access to food and water. All procedures involving mice, e.g., handling, administration of hormones for superovulation of females were conducted at the PRAAL Animal Facility, while procedures involving oocyte manipulation, e.g., oocyte collection, oocyte insemination and embryo culture up to blastocyst were performed at Embryotools' laboratories.

A total of 10 mL of *Fertilo* IVM media, consisting of MediCult IVM Base Media (CooperSurgical Origio), 10 mg/mL human serum albumin (HSA) (CooperSurgical Origio), 75 mIU/mL recombinant follicle stimulating hormone (rFSH) (Sigma), 100 mUI/mL human chorionic gonadotropin (hCG) (Sigma), and 500 ng/mL androstendione (Sigma), and 10 mL of IVM control media, consisting of MediCult IVM Base Media (CooperSurgical Origio), 10 mg/mL HSA (CooperSurgical Origio), 75 mIU/mL rFSH (Sigma), 100 mUI/mL hCG (Sigma), and 500 ng/mL androstenedione (Sigma), were prepared and stored at 4°C until use. Plating dishes were prepared 16-24 hours prior to oocyte culture to allow for equilibration. The wells of a universal GPS dishes (UGPS-010, Cooper)

were prepared with 50 μL LAG media, 100 μL *Fertilo* IVM media, 100 μL IVM control media, or 50 μL *Fertilo* IVM media/ IVM control media for wash droplets. Then, 12 mL of mineral oil (Kitazato) was used to overlay droplets. All dishes were incubated overnight at 37°C with CO2 set for a pH of 7.2-7.4 and 5% O2.

On the day of oocyte culture, *Fertilo* OSCs were seeded 2-5 hours before co-culture. To thaw *Fertilo* OSCs, one OSC cryovial was removed from liquid nitrogen storage and placed upright into a 37°C water bath or dry bead bath to incubate for 2-3 minutes or until ice dissolved. Then, 400 μL of pre-warmed *Fertilo* IVM media was added to the vial and the cells were mixed by pipetting. After, 500 μL of the cell suspension was added to a 1.5 mL Eppendorf tube and centrifuged at 300 x G for 5 minutes at room temperature (RT). The supernatant was then removed and the cells were gently resuspended in another 400 μL pre-warmed *Fertilo* IVM media. Following centrifugation at 300 x G for 5 minutes at RT, most supernatant was removed while ensuring not to disturb the pellet. The cells were then resuspended in pre-warmed *Fertilo* IVM media to 100,000 OSCs per 50 μL according to batch specifications provided in the *Fertilo* Certificate of Analysis. Then, the plating dishes were removed from the incubator and 50 μL of media was removed from the wells with *Fertilo* IVM media. After gently pipetting the cell suspension, 50 μL of OSCs were added to the wells with *Fertilo* IVM media, for a concentration of 100,000 OSCs in 100 μL media. The plate was then placed back into the 37°C incubator for at least 2 hours until oocyte seeding.

Fresh immature mouse oocytes at the germinal vesicle (GV) stage were collected from the ovaries of hybrid (B6/CBA) females between 6 and 8 weeks of age stimulated with 7.5 IU pregnant mare serum gonadotropin (PMSG) 48 hours before retrieval. GVs with cumulus cells were then randomly split between the *Fertilo* IVM group or the IVM control group. Oocytes were then plated and the plates were incubated at 37°C for 18 hours for IVM. After IVM, oocytes were stripped using hyaluronidase (H3884-50MG, Sigma) and assessed for maturity. Mature oocytes with first polar body extrusion were selected for intracytoplasmic sperm injection (ICSI). Fresh sperm from B6/CBA hybrid strain mice was obtained in a microdroplet of culture medium and cultured for 15 minutes at 37°C, 5% CO2, and 5% O2. After incubation, 3 μL of the concentrated sperm solution was further diluted in a 150 μL droplet of the same culture medium. ICSI was performed using a piezo drill-based protocol optimized for the mouse species. Briefly, mouse sperm heads were isolated from the tail and injected into the mature oocytes. Following injection, the oocytes were thoroughly washed and cultured until day 5 (120 hours) in benchtop incubators at 37°C, 5% CO2, and 5% O2. Embryo development was monitored until the last day of culture, at which point images of each embryo were acquired.

Clinical evaluation

The clinical analysis was performed as the first-in-human study to demonstrate the application and outcomes of *Ferilo* utilization in a clinical context. Oocyte search was conducted according to standard IVM procedures. Briefly, follicular aspirate was kept warm and passed over a 70 micron cell strainer to separate and filter blood from potential cumulus oocyte complexes (COCs). The filter was then overturned and the COCs were released into a search media lacking heparin (ASP) via dipping and pipette expulsion. COCs were identified under stereomicroscope and transferred to a warmed holding droplet until all oocytes had been found. Typical IVM oocytes were highly compact, containing one to a few layers of cumulus enclosure. Expanded COCs were rarely identified, due to the use of an hCG trigger, and proper monitoring during stimulation was implemented to keep the leading follicle under 12 mm.

All COCs were cultured in either *Fertilo* or Traditional IVM for 30 hours. IVM culture was performed the same for both conditions. Briefly, IVM was performed in Birr 4+8 dishes using microdroplet culture. Culture droplets were 100 μL and were utilized for the culture of up to 5 COCs. Traditional IVM utilized the IVM basal media containing supplementation with 75 mIU/mL rFSH (Gonal-F), 200 mIU/mL hCG (Ovidrel), and 10 mg/mL HSA. For OSC-IVM, the same IVM basal media was utilized and performed as previously described. In OSC-IVM, 100,000 viable OSCs were supplemented into each 100 μL droplet the day of oocyte retrieval. All culture media plates were prepared the day before oocyte retrieval to allow for equilibration under IVF grade oil in 37°C incubators with CO2% to yield a pH of 7.2 to 7.4 and 5% O2. For OSC-IVM, the OSCs (*Fertilo*) were delivered to the clinic under liquid nitrogen vapor shipment and stored in liquid nitrogen until use. For each application, at least two vials of OSCs were prepared to enable treatment of up to 30 COCs across 6 culture droplets, with each droplet containing 100,000 OSCs. Briefly, the day of oocyte retrieval OSCs were thawed at 37°C for 2-3 minutes, gently resuspended using IVM basal media, and centrifuged at 300 x G for 5 minutes to pellet the cells. Supernatant was fully removed to eliminate residual cryoprotectant (Cryostore CS10) and the cells were resuspended using a defined volume of equilibrated complete IVM media described above. A cell count was performed using a cell counting chamber and 100,000 viable OSCs were supplemented into each droplet by replacement of the corresponding volume with the cell suspension. The dishes were incubated for at least 30 minutes prior to oocyte co-culture to allow for re-equilibration. All COCs were washed in IVM basal media and moved into the culture droplets of either OSC-IVM or Traditional IVM and cultured for 30 hours in a 37°C incubator at a %CO2 to achieve a pH of 7.2 to 7.4 and 5% O2.

Mature oocytes were fertilized using ICSI and cultured in group or single culture using single-step embryo culture medium. Assessment of the fertilization rate was performed at 16-18 hours post-ICSI, then at Days 3, 5, 6, and 7 post IVM. A standardized embryo grading system based on the classification system by Gardner & Schoolcraft (Gardner classification) was used on Days 5-7. Embryos that did not meet their respective checkpoints were discarded and blastocysts of freezable quality (Gardner grade 3BB or greater) underwent vitrification (Kitazato). Embryos were hatched using laser-assisted hatching and underwent trophectoderm biopsy prior to vitrification on the day of freezing. Preimplantation genetic testing for aneuploidy (PGT-A) was performed using microarray-based or SNP-based NGS analysis in local laboratories. Only embryos considered euploid were utilized for transfer. Low grade mosaicism,

Please cite this article in press as: Paulsen et al., Development of human induced pluripotent stem cell-derived ovarian support cells as a clinical-grade product for *in vitro* fertilization, Cell Stem Cell (2025), https://doi.org/10.1016/j.stem.2025.12.020

after consultation with a geneticist, were utilized for transfer depending on patient preference. The highest quality embryo was thawed later for frozen embryo transfer (FET) within 2 months of cryopreservation. Only single blastocyst transfers were allowed and all transfers were FET cycles.

For uterine priming, starting on the first day of menses, subjects received 2 mg oral estradiol treatment twice daily with an optional 100 μg patch replaced every three days until the endometrial thickness was ≥7 mm. Progesterone was then administered at 50 mg intramuscular once daily to prepare for ET or via a combination of intravaginal (800 mg) and subcutaneous progesterone. Progesterone could be increased to 100 mg daily if clinically indicated due to bleeding or a low progesterone level.

Following ET, serum beta human chorionic gonadotropin (BHCG) levels were measured 10-14 days post-transfer and followed until an appropriate rise was confirmed (2-3 days following 1st confirmation), indicating a biochemical pregnancy.

Transvaginal ultrasounds were performed at 4-6 weeks gestation to establish the presence of a gestational sac, indicating clinical pregnancy, and a follow-up ultrasound was performed at 8-12 weeks of gestation to confirm ongoing pregnancy with a normal, healthy heartbeat. If a subject became pregnant, P4 and E2 administration were continued for up to 8-12 weeks of gestation.

The site staff followed-up with subjects who had an ongoing pregnancy after discharge from the clinic to obtain a second trimester pregnancy ultrasound record (Week 20-24 Anomaly scan performed by an OBGYN) and serious adverse events (SAE) collection via a second trimester in person visit. Additionally, the clinic obtained birth data from the patient. Adverse events of special interest (AESI) such as response to stimulation and retrieval, ovarian hyperstimulation syndrome (OHSS), pregnancy loss, fetal anomalies, pregnancy complications, birth weight, birth defects, and neonatal complications were collected. For the purposes of this evaluation, only the outcomes of the first embryo transfer were considered in the rates.

QUANTIFICATION AND STATISTICAL ANALYSIS

A p-value <0.05 was considered statistically significant in all cases, and all data analyses were conducted using GraphPad Prism software (GraphPad Software, San Diego, CA, USA) unless otherwise stated in the figure legends. Specific statistical details about experiments can be found in the relevant figure legends. Information about the statistical analysis performed for the DoE can be found in the relevant section above.

In the clinical evaluation second phase (comparative), for all demographic comparisons between arms, an unpaired, two-tailed T-test was performed. Data from comparison of the demographic characteristics of patients can be found in Table S6. Both phases of the clinical evaluation were designed as a small cohort, observational analysis to provide preliminary evidence of safety and efficacy at the embryological level and was not powered for determination of superiority or non-inferiority for *in vivo* endpoints after embryo transfer.